Control of Spatial Orientation of the Angular Vestibuloocular Reflex by the Nodulus and Uvula

SUSAN WEARNE, THEODORE RAPHAN, AND BERNARD COHEN
Departments of Neurology and Biophysics and Physiology, Mount Sinai School of Medicine, New York 10029; and Computer and Information Sciences, Brooklyn College of the City University of New York, Brooklyn, New York 11210

Wearne, Susan, Theodore Raphan, and Bernard Cohen. Control of spatial orientation of the angular vestibuloocular reflex by the nodulus and uvula. *J. Neurophysiol.* 79: 2690–2715, 1998. Spatial orientation of the angular vestibuloocular reflex (aVOR) was studied in rhesus monkeys after complete and partial ablation of the nodulus and ventral uvula. Horizontal, vertical, and torsional components of slow phases of nystagmus were analyzed to determine the axes of eye rotation, the time constants (Tcs) of velocity storage, and its orientation vectors. The gravito-inertial acceleration vector (GIA) was tilted relative to the head during optokinetic afternystagmus (OKAN), centrifugation, and reorientation of the head during postrotatory nystagmus. When the GIA was tilted relative to the head in normal animals, horizontal Tcs decreased, vertical and/or roll time constants ($Tc_{vert/roll}$) lengthened according to the orientation of the GIA, and vertical and/or roll eye velocity components appeared (cross-coupling). This shifted the axis of eye rotation toward alignment with the tilted GIA. Horizontal and vertical/roll Tcs varied inversely, with Tc_{hor} being longest and $Tc_{vert/roll}$ shortest when monkeys were upright, and the reverse when stimuli were around the vertical or roll axes. Vertical or roll Tcs were longest when the axes of eye rotation were aligned with the spatial vertical, respectively. After complete nodulo-uvulectomy, Tc_{hor} became longer, and periodic alternating nystagmus (PAN) developed in darkness. Tc_{hor} could not be shortened in any of paradigms tested. In addition, yaw-to-vertical/roll cross-coupling was lost, and the axes of eye rotation remained fixed during nystagmus, regardless of the tilt of the GIA with respect to the head. After central portions of the nodulus and uvula were ablated, leaving lateral portions of the nodulus intact, yaw-to-vertical/roll cross-coupling and control of $Tc_{vert/roll}$ was lost or greatly reduced. However, control of Tc_{hor} was maintained, and Tc_{hor} continued to vary as a function of the tilted GIA. Despite this, the eye velocity vector remained aligned with the head during yaw axis stimulation after partial nodulo-uvulectomy, regardless of GIA orientation to the head. The data were related to a three-dimensional model of the aVOR, which simulated the experimental results. The model provides a basis for understanding how the nodulus and uvula control processing within the vestibular nuclei responsible for spatial orientation of the aVOR. We conclude that the three-dimensional dynamics of the velocity storage system are determined in the nodulus and ventral uvula. We propose that the horizontal and vertical/roll Tcs are separately controlled in the nodulus and uvula with the dynamic characteristics of vertical/roll components modulated in central portions and the horizontal components laterally, presumably in a semicircular canal-based coordinate frame.

INTRODUCTION

The angular vestibuloocular reflex (aVOR) exhibits the property of spatial orientation. During nystagmus induced by rotation of the subject or surround, the yaw axis component of slow-phase velocity tends to align with gravity or with the gravito-inertial acceleration vector (GIA) (Angelaki and Hess 1994a,b; Dai et al. 1991; Harris 1987; Harris and Barnes 1987; Raphan and Cohen 1986; Raphan et al. 1992, 1996; Raphan and Sturm 1991; Wearne et al. 1996, 1997a,b). Alignment of the eye velocity vector with the GIA has been modeled by three processes: a reduction in the time constant of the dominant horizontal component, an increase in the torsional and/or vertical time constants, and the appearance of orthogonal vertical or torsional ''cross-coupled'' eye velocity (Dai et al. 1991; Raphan and Cohen 1996; Raphan et al. 1992; Raphan and Sturm 1991).[1] We have shown that the velocity storage mechanism in the vestibular system is responsible for spatial orientation of the aVOR, and that the direct visual and vestibular pathways do not orient eye velocity to the GIA (Wearne et al. 1997a). The study of the spatial orientation of the aVOR is therefore essentially a study of the three-dimensional characteristics of velocity storage. Because velocity storage is activated by somatosensory input in both monkey (Solomon and Cohen 1992) and humans (Bles et al. 1984), this type of spatial orientation is likely to be important for postural and gaze stabilization during angular locomotion (Cohen 1998).

Behavioral, lesion, and stimulation studies indicate that the nodulus and uvula control the horizontal time constant of velocity storage, one element in determining its spatial orientation. The horizontal aVOR time constant is reduced when the head is reoriented relative to gravity during postrotatory nystagmus (tilt dumping), both in humans (Benson 1974; Fetter et al. 1992) and in monkeys (Angelaki and Hess 1994a; Merfeld 1995; Merfeld et al. 1993; Raphan et al. 1981; Solomon and Cohen 1994; Waespe et al. 1985). The horizontal time constant is also reduced when subjects view a relative stationary visual surround during vestibular nystagmus or optokinetic afternystagmus (OKAN; light dumping) (Cohen et al. 1977, 1981; Waespe et al. 1983, 1985). Electrical stimulation of the nodulus and lobule 9d of the ventral uvula reproduces this reduction (Solomon and Cohen 1994). Both tilt dumping and light dumping are lost after ablation of the nodulus and uvula (Angelaki and Hess 1994a, 1995; Waespe et al. 1985).

The nodulus and ventral uvula are likely also to be involved in producing the changes in vertical and/or torsional

[1] We define spatial orientation of the aVOR as alignment of the eye velocity vector with gravito-inertial acceleration (GIA). GIA is the vector sum of gravitational and inertial accelerations. Cross-coupling is the appearance of vertical and/or torsional eye velocities in response to tilts of the GIA during yaw axis stimulation.

0022-3077/98 $5.00

components that tilt the eye velocity axis during spatial orientation. The cortex of the nodulus and uvula has been divided into parasagittal zones comprising strips of Purkinje cells, innervated by subnuclei of the inferior olive (Voogd 1964, 1969; Voogd et al. 1996; Voogd and Bigaré 1980). There are both visual (optokinetic) and vestibular climbing fiber afferents to the nodulus of the rabbit, and their sensitivity axes are aligned approximately with the axis of one of the three semicircular canals (Barmack and Shojaku 1992, 1995; Kano et al. 1990; Wylie et al. 1994). (The sensitivity axis of a neuron is that axis around which rotation causes a maximal modulation of its firing rate.) These axes, derived from physiological studies in the rabbit, are shown projected onto a monkey head in Fig. 1*B*. Activity induced by yaw optokinetic stimulation and nystagmus (OKN) about a vertical axis [VA (Yaw) OKN] is processed in the caudal dorsal cap (cdc), whereas activity related to optokinetic stimulation about an axis parallel to that of the ipsilateral anterior canal [horizontal axis, HA (135°) OKN] reaches the cerebellar cortex through the rostral dorsal cap (rdc) and ventrolateral outgrowth (vlo) (Balaban and Henry 1988; Barmack and Shojaku 1992; Graf et al. 1988; Kano et al. 1990; Katayama and Nisimaru 1988; Leonard et al. 1988; Simpson et al. 1981; Takeda and Maekawa 1984). Vestibular signals aligned approximately with the anterior and posterior canal axes [AC and PC (135°) VOR signals] project from the beta nucleus of the inferior olive (Alley et al. 1975; Balaban and Henry 1988; Barmack et al. 1993a; Barmack and Shojaku 1992, 1995; Katayama and Nisimaru 1988; Shojaku et al. 1991). Utricular signals project from the dorsomedial cell column (DMCC) (Barmack and Fagerson 1994) and the beta nucleus (Barmack et al. 1989, 1993b). As yet, no lateral canal-related signals have been found in the inferior olive or in climbing fiber responses (Barmack and Shojaku 1992, 1995).

Unlike the rabbit, no physiological studies relating zonal organization to function have been performed in rhesus monkey. Anatomic studies, however, have demonstrated a similar zonal organization in the rhesus monkey to that of the rabbit (Voogd et al. 1996). Four sagittal zones have been distinguished, based on four white matter compartments innervated by discrete subnuclei of the contralateral inferior olive. The most medial zone (Zone 1) extends from the midline to 0.8 mm lateral in the nodulus and uvula. It receives composite climbing fiber input from the beta nucleus medially and the lateral caudal dorsal cap. If it is assumed that the same canal-, otolith-, and OKN-related information is present in the inferior olive of the monkey as in the rabbit, Zone 1 has horizontal axis [vertical canal, HA (135°) VOR] and otolith (β) as well as yaw axis representation [cdc; VA (Yaw) OKN]. The second zone (Zone 2) extends from 0.8 to 2.4 mm in the nodulus and uvula, and forms the lateral limits of the vermis over the posterior surface of the cerebellum. Zone 2 was labeled from injections that included the ventrolateral outgrowth, rostral beta, and rostral medial accessory olive (rMAO) in rhesus monkey (Voogd et al. 1996). Input to this zone from vlo and from rostral β is related in the rabbit to HA (135°) OKN, HA (135°) VOR, and the utricle. Zone 3, innervated by the caudal dorsal cap in the monkey, would receive information about yaw axis OKN [VA (Yaw) OKN]. It extends from 2.4 to 3.2 mm in the nodulus and is restricted to the nodulus. Zone 4 extends from 3.2 to 4 mm lateral. Its olivocerebellar afferents are currently unidentified in rhesus monkey, but by analogy with the lateral zone in rabbit, probably include the DMCC and rMAO (Balaban and Henry 1988; Katayama and Nisimaru 1988; Tan et al. 1995). We have adopted the classification of Voogd et al. (1996) for the animals in our series, and these four zones are represented in Figs. 4 and 18.

It has been postulated that an important function of the nodulus and ventral uvula of the rabbit is to determine three-dimensional spatial orientation (Barmack and Shojaku 1992). The same is likely true for the monkey. Accordingly, complete or partial nodulo-uvulectomy was reported to impair the dynamics of the low-frequency torsional aVOR in the monkey, leaving the vertical aVOR relatively unaffected (Angelaki and Hess 1994a, 1995). Preliminary results following similar nodulo-uvular lesions, however, suggest that the nodulus and uvula control aVOR dynamics in all dimensions (Wearne et al. 1996).

The purpose of this study was to characterize the three-dimensional behavior of eye velocity during paradigms that shift the GIA relative to the head before and after partial and complete lesions of the nodulus and uvula. Constant velocity centrifugation provides a robust technique for shifting the GIA vector relative to the head, and reorientation of eye velocity axes to the GIA has not been studied after nodulo-uvulectomy with centrifugation. In addition to centrifugation, we utilized previously studied paradigms, such as OKAN in tilted positions, tilt dumping, and light dumping. We wished to determine whether the nodulus and uvula control spatial orientation of the aVOR around all axes. In the course of this study, it became apparent that processes related to control of time constants around different axes could be separated and localized to different regions of the nodulus and uvula. A preliminary report has been presented (Wearne et al. 1996).

METHODS

Juvenile rhesus monkeys (*Macaca mulatta;* weight 3–4 kg) were used in these studies. Quantitative data came largely from two animals with representative complete and partial lesions (*M9312* and *M9303*), but relevant results from five other monkeys with complete (*M1107*, *M1152*, and *M1153*) and partial lesions (*M1173* and *M1175*) from previous studies (Cohen et al. 1992; Waespe et al. 1985) were reanalyzed to expand the database. The experiments conformed to the *Principles of Laboratory Animal Care* (NIH Publication 85-23, Revised 1985), and were approved by the Institutional Animal Care and Use Committee.

Surgical procedures

Animals were prepared initially under anesthesia with a frontal plane coil to record horizontal and vertical eye position (Judge et al. 1980; Robinson 1963). A roll coil was threaded around the superior rectus muscle on top of the eye to record roll eye position (Dai et al. 1994; Yakushin et al. 1995). Bolts implanted on the skull provided painless head stabilization during experiments. The animals were allowed to recover from anesthesia and received baseline testing. At a later date, they were reanesthetized, and a 25% solution of mannitol (250 mg/ml) was administered to a dose of 1 gm/kg to reduce brain vascularity and edema. Under gas inhalation anesthesia, the dura and pia mater were opened, and the

cerebellum was exposed. The secondary fissure was identified, and a horizontal dissection plane was established below the secondary fissure, between lobules 9a and 9b. The rostral extension of this plane led to the fourth ventricle just caudal to the fastigial nucleus. Partial lesions were confined to the central vermis. The nodulus (lobule 10) and ventral uvula (sublobules 9c and 9d) were aspirated from the midline to the lateral margins of the uvula (approximately ±2 mm). Complete nodulo-uvulectomy was performed by extending the dissection laterally in its rostral portions to include the lateral 2 mm of the nodulus (Madigan and Carpenter 1971; Snider and Lee 1961). More of the dorsal uvula (sublobules 9a and 9b) was generally removed in the complete than the partially lesioned animals. Bleeding was generally slight and was controlled with cautery. Vomiting, which can occur postoperatively after nodulo-uvulectomy (Cohen et al. 1992; Waespe et al. 1985), was prevented by prophylactic administration of promethazine HCl (2 mg/kg). Animals also received analgesics and antibiotics postoperatively. The animals were initially posturally unstable, but this gradually disappeared over the next several weeks.

Stimulation apparatus

Testing began ~1 wk after operation and continued for 12–36 mo. Eye movements were induced by optokinetic stimulation, by angular acceleration about an earth vertical axis with the animal either centered or at a 25-cm radius from the axis of rotation, or by rapidly reorienting the animal during postrotatory vestibular nystagmus. The stimulator (Neurokinetics, Pittsburgh, PA), has been described previously (Wearne et al. 1996, 1997a,b). In brief, it had three independently controlled, gimbaled axes of rotation: an outer horizontal axis, a nested yaw axis, and a doubly nested inner pitch-roll axis. The yaw and pitch-roll axes were enclosed in a light-tight, optokinetic sphere, 109-cm diam, with 10° vertical black and white stripes on the inside. The axis of the OKN sphere, which was also independently controlled, was collinear with the yaw axis. When the OKN sphere rotated, it produced full field motion that induced OKN and OKAN.

Monkeys were seated in a primate chair with the head and eyes centered in the field coils. The animals could be positioned either with the head centered with respect to each rotation axis or at the end of the centrifuge arm, directing centripetal acceleration along the interaural or the nasooccipital axes. With the monkey erect, the yaw axis was aligned with gravity, and the horizontal stereotaxic plane was aligned with the gravitational horizontal. Thus the lateral semicircular canals were tilted up ~30° from the earth horizontal plane during the experiments (Blanks et al. 1985; Yakushin et al. 1995).

Coordinates and notation

The three-dimensional components of the vestibular stimuli and oculomotor responses were referenced to the right-handed Cartesian coordinate system shown in Fig. 1*A*. The *X*-, *Y*-, and *Z*-axes denote the interaural (positive left), nasooccipital (positive backward), and dorsoventral (positive up) axes of the head, respectively. Three-dimensional eye orientation is represented as Euler angles using the Fick rotation convention.[2] The symbols, ϕ, θ, and ψ, represent rotations about the *Z*-axis, the rotated *X*-axis, and the doubly rotated *Y*-axis (visual axis). These angular deviations from the reference position will be referred to as horizontal, vertical, and roll eye positions, respectively. The components of the eye velocity vector in head coordinates, symbolized by $\omega = [\omega_X, \omega_Y, \omega_Z]$ that denoted vertical, torsional, and horizontal components, were obtained directly from the Euler angles and their derivatives (Goldstein 1980; Yakushin et al. 1995). Positive directions for the rotations are in accordance with the right-hand rule (Fig. 1*A*).

To provide a basis for comparison, the coordinate frame determined from studies in the rabbit (Barmack et al. 1993b; Barmack and Shojaku 1992; Wylie et al. 1994) has been superimposed on the coordinate frame utilized in this study on the monkey (Fig. 1*B*). The axes of the ipsilateral anterior and posterior canals (AC and PC), are oriented at ~45 and 135° from the nasooccipital axis of the head. The vertical axis (VA) is aligned with the +*Z* head axis, whereas the positive pole of the horizontal axis (HA) (135°) is rotated counterclockwise about the +*Z*-axis by 135° from the forward-pointing pole of the nasooccipital (−*Y*) axis. The VA and HA axes are those axes about which rotation of the head or visual surround maximally activates climbing fibers and complex spike responses of Purkinje cells (Barmack and Shojaku 1992; Kano et al. 1990; Simpson and Alley 1974; Wylie et al. 1994). Thus the VA axis aligns approximately with the axis of the lateral canals, and the HA (135°) axis aligns with the axis of the ipsilateral (left) anterior canal and contralateral (right) posterior canal.

Calibration of eye position

Eye orientation was measured using the implanted scleral search coils. The normal to the frontal coil on the implanted eye was aligned with the visual axis. Portions of the frontal coil voltages were subtracted from the roll coil voltages to remove cross-talk as the upright animal was rotated around a spatial vertical axis. To calibrate eye position in untrained monkeys, we made use of the fact that Listing's plane is aligned approximately with the coronal head plane and is independent of the initial reference position from which eye position axes are calculated (Helmholtz 1866; Tweed and Vilis 1990). We assumed that the average coil voltages during spontaneous positions of fixation while the animal made saccades for 15–30 s in light correspond to the straight ahead eye position with zero roll. This assumption is consistent with data obtained in trained and calibrated monkeys for a large range of saccades in light and dark (van Opstal et al. 1995). When the eye is in this orientation, the visual axis is aligned with the $-e_Y$ axis of the head frame. To a good approximation, this aligns with the stereotaxic coordinate frame of the head, which we physically aligned with the axes of the horizontal and vertical field coils. More complete details of the calibration of eye orientation are presented in Yakushin et al. (1995).

Experimental protocol

The order of testing was independently randomized for each monkey, and repeated measures were performed on each experimental condition. Amphetamine sulfate (0.3 mg/kg) was given 30 min before testing to maintain alertness. Monkeys were rotated in yaw to habituate the time constant of velocity storage to some stable value. This ensured that effects of habituation during the experiments would not significantly influence the experimental results (Cohen et al. 1992). As a result the time constant and initial value of OKAN for the upright position remained approximately constant throughout the period of testing. The horizontal OKAN time constant in the upright position was ~15–25 s, depending on the monkey. Intrasubject variability remained low throughout the period of testing.

Eye movements were induced in three stimulus paradigms. The animals were given steps of yaw axis optokinetic stimulation at 60°/s and 90°/s, lasting 30 s (Fig. 1*C*). This induced horizontal OKN and OKAN. OKN was elicited in light and OKAN in darkness. Tilts were left or right ear down (LED or RED) with regard to gravity at angles of 0, 17, 36, 45, 52, and 90°. The GIA was tilted by eccentric constant velocity rotation on a centrifuge in

[2]The Fick rotation convention parameterizes any three-dimensional rotation as three sequential rotations about three nonorthogonal axes, *Z*, the rotated *X*, and the final *Y* (visual axis) in that order.

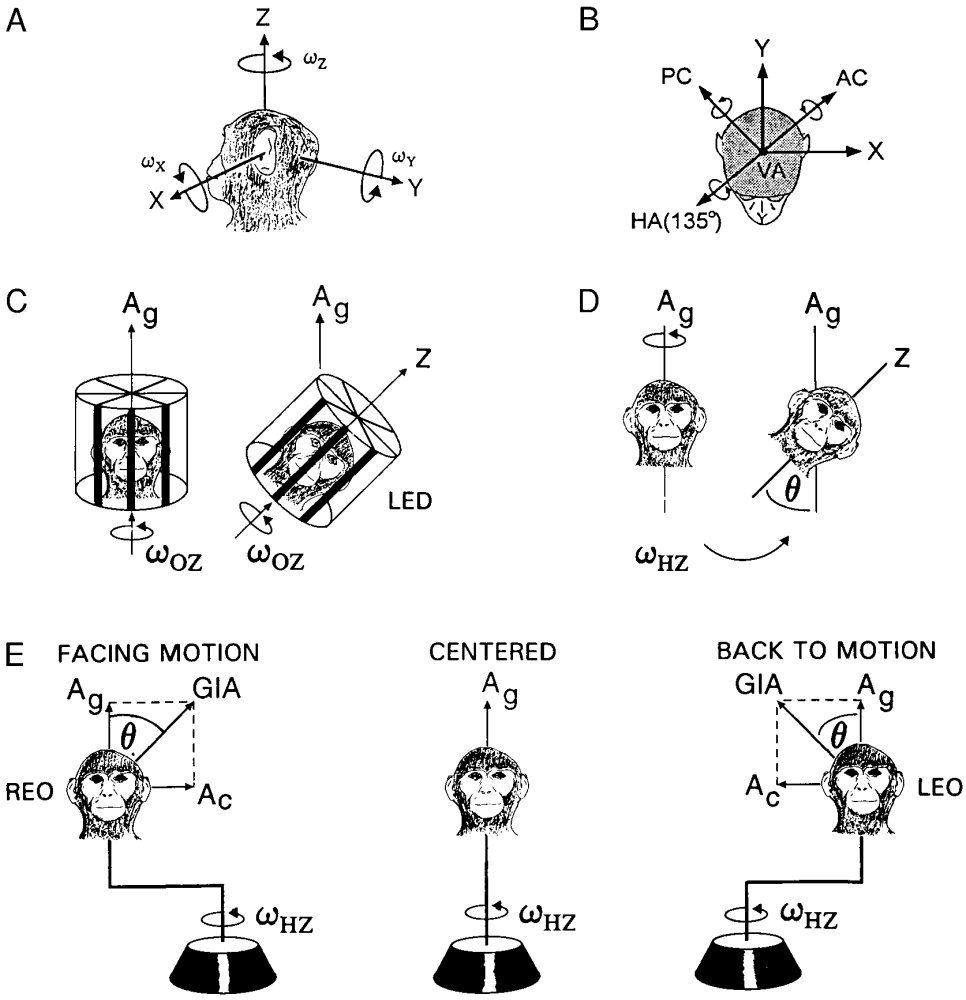

FIG. 1. *A*: right-handed coordinate frame to which components of the eye velocity vector are referred. Positive direction of rotation about each axis is defined according to the right hand rule, as leftward yaw ($+\omega_Z$), downward pitch ($+\omega_X$) and counterclockwise roll ($+\omega_Y$), from the animal's point of view. *B*: relation between the head reference frame used to describe 3-dimensional eye movements and maximal sensitivity axes for visual modulation of neurons in the left nodulus and right inferior olive of the rabbit (modified from Simpson and Graf 1985). The excitatory direction for visually and vestibularly induced complex spike responses of Purkinje cells in the left nodulus of the rabbit is indicated by the curved arrows about axes VA and HA (135°) (Barmack and Shojaku 1992). *C–E*: paradigms used to tilt the gravito-inertial acceleration vector (GIA) relative to the head during optokinetic or vestibular nystagmus. *C*: continuous tilts of GIA induced during optokinetic afternystagmus (OKAN) with the head upright and tilted left ear down (LED). A_g is the equivalent acceleration due to gravity. The angular velocity of the surround, along the *Z*-axis of the head, is given by ω_{OZ}. *D*: reorientation of the head with respect to the GIA during postrotatory nystagmus with the GIA equivalent to the vector of gravitational acceleration (A_g). The angular velocity of the head along the *Z*-axis is given by ω_{HZ}. During postrotatory nystagmus, the animal is tilted in the roll plane by the angle θ, shifting the GIA relative to the head. *E*: centrifugation facing motion, centered and back to motion. Centripetal acceleration is indicated as A_c. The vector sum of A_g and A_c is the GIA vector. The angle between A_g and the GIA in the roll plane is given as θ_R. For $+\omega_{HZ}$ rotation, the animal was oriented right ear out when facing motion, and left ear out (LEO) when back to motion. An analogous stimulus paradigm was given for $-\omega_{HZ}$ rotation, with left ear out when facing motion and right ear out (REO) when back to motion.

darkness, either facing the direction of motion (Fig. 1*E*, *left*), with back to the motion (Fig. 1*E, right*) or facing radially, nose-in or nose-out (Fig. 11*B*). Centrifugation was called tangential when facing or back-to-motion and radial when nose-in or nose-out. The centrifuge was accelerated at 40°/s^2 to a final angular velocity of 400°/s. This generated a maximum interaural centripetal acceleration of 1.24 g and tilted the GIA vector, the sum of gravitational (A_g) and centripetal (A_c) accelerations, by 51° with respect to gravity. The final stimulus velocity was maintained for at least 120 s. For $+Z$ rotation, animals were right ear out (REO) when facing motion (Fig. 1*E*, *left*) and left ear out (LEO) when back to motion (Fig. 1*E*, *right*). For $-Z$ rotation, these conventions were reversed. For facing and back to motion centrifugation, A_c was directed along the interaural axis, and the GIA tilted dynamically in the roll plane of the head, through an angle (θ) that increased with the angular velocity of the centrifuge. Animals were also rotated about a centered axis (Fig. 1*E*, *middle*).

In addition, animals were tilted with respect to the GIA by reorienting them about the roll or pitch axes during postrotatory nystagmus in darkness (tilt dumping). Nystagmus was induced by rotation at 60°/s about a spatial vertical axis. When the per-rotatory nystagmus had decayed to zero, rotation was stopped, inducing postrotatory nystagmus. Two seconds later, the head was rapidly reoriented by rotating the animal about a spatial horizontal axis

TABLE 1. *Horizontal and vertical VOR gains and time constants for nodulectomy animals*

	Complete				Partial		
Lesion: Lobules 9d and 10	*M9312*	*M1107**	*M1152**	*M1153**	*M9303*	*M1173**	*M1175**
Horizontal OKAN time constant, s							
Pre	12 ± 2	21 ± 2	29 ± 13		15*	14**	16 ± 3
Post	24 ± 6	37 ± 9	57 ± 19		16†	17 ± 3	14 ± 2
Horizontal aVOR time constant, s							
Pre	12 ± 2	36 ± 9	32 ± 8	20**	14 ± 1	29**	24**
Post	22 ± 4	60 ± 11	43 ± 9	75†	12 ± 1	26 ± 4	22 ± 2
Vertical aVOR time constant, s							
Pre	10 ± 3	19 ± 3	18 ± 5		11*		
Post	5 ± 2	6 ± 0.5	6†		2 ± 1		
Perodic alternating nystagmus (PAN) period, s							
Pre	+	+	+	+	−	−	−
Post	152	245	250	250	−	−	−
Tilt dump							
Pre	+	+	+	+	+	+	+
Post	−	−	−	−	+	+	+
Light dump							
Pre	+	+	+	+	+	+	+
Post	−	−	−	−	+	+	+

Values are means ± SD for 4–10 measurements. Comparison of findings in animals with complete and partial lesions. Horizontal and vertical time constants were obtained during rotation of the subject or surround at 60°/s. The horizontal values represent averages of left and right eye velocity. For *M9312* and *M9303*, the larger of the standard deviations for the right and left measurements is listed. Vertical time constants were measured from upward eye velocity. For tilt and light dumps, the plus sign indicates that the horizontal velocity storage time constant was reduced after operation by either tilt or exposure to a stationary visual surround (see METHODS). In *M9312* and *M9303*, a double time constant technique was used to estimate the central (velocity storage) time constant of the aVOR responses. VOR, vestibuloocular reflex; OKAN, optokinetic afternystagmus; aVOR, angular VOR. * First value (recorded before habituation). ** Single area time constant estimate was used. † Single value.

(Fig. 1*D*, *right*). In the normal monkey, this causes a reduction in the horizontal time constant (tilt dumping) and the appearance of concurrent vertical and/or torsional velocities (cross-coupling).

The ratio of the recovery velocity to the velocity just before exposure to the light is a measure of the effects of visual suppression on the velocity storage integrator (Cohen et al. 1977) and was compared in the normal, completely lesioned and partially lesioned animals. These results are reported in Table 1 in which dumping was considered absent if the recovery velocity reached levels within 20% of those expected as a result of decline of eye velocity in darkness, plus losses due to visual feedback, determined from the rising time constant (Raphan et al. 1979; Waespe et al. 1983, 1985). If the velocity profile was reduced by >20% from the expected level, then it was labeled as positive (+). For tilt dumping, the plus sign in Table 1 indicates that the horizontal velocity storage time constant was reduced by tilt dumps, and the minus sign indicates a lack of effect. Dumping was considered absent in response to tilt (−) if the time constant of decline in horizontal slow-phase velocity was consistently within 30% of the time constant recorded in the upright position.

Data acquisition and processing

Eye position and photocell data were sampled at a rate of 600 Hz per channel. Before sampling, the eye position data were prefiltered by an 8-pole Butterworth filter with a cutoff corner frequency of 30 Hz. Slow-phase eye velocity was obtained by calculating the vector of eye velocity in head coordinates and removing saccades, using an order statistic filter (Engelken and Stevens 1990, 1991). Slow-phase velocities were analyzed from the onset of OKAN to the point where the yaw axis eye velocity decayed to zero. OKAN time constants were estimated by fitting a single exponential function to the decaying portion of eye velocity starting 2 s after the end of stimulation (Cohen et al. 1977). During steps of angular velocity for *M9312* and *M9303*, velocity storage time constants were estimated by fitting a sum of two exponential functions to the decaying portion of eye velocity (Raphan et al. 1979). The cupula time constant was constrained to 4 s (Goldberg and Fernández 1971), and the initial integrator state was constrained to be zero. Whenever a single time constant is quoted for these animals, it is the central or velocity storage time constant. If secondary nystagmus appeared during measurement of aVOR time constants, the offset due to overshoot was subtracted before time constants were fitted. Time constants for the other animals were determined from paper records by dividing the area under the slow-phase velocity envelope by the initial jump in velocity (Raphan et al. 1979). Animals in whom a single area time constant estimate was used are marked with double asterisks in Table 1. The direction of nystagmus is denoted in the figures and the text by the direction of the slow-phase velocity.

Slow-phase velocities during centrifugation were analyzed from the end of the angular acceleration until the nystagmus had decayed to zero. Slow-phase velocity was related to the eigenvalues and eigenvectors of the velocity storage system matrix (Raphan and Sturm 1991) by fitting the best tangent line to the three-dimensional eye velocity vector starting 10 s after reaching constant angular head velocity (Wearne et al. 1997a,b). Because the decay of the eye velocity trajectory approaches the yaw axis eigenvector in the limit (Raphan et al. 1992; Raphan and Sturm 1991), this tangent line is a close approximation to the eigenvector. The magnitude of axis shift in the head coordinate frame was computed as the angular difference between the yaw eigenvector and the *Z*-axis of the head. The three-dimensional tangent line was then projected into each cardinal head plane, and the angle made by this projection and the *Z*-axis was computed in each plane. Goodness of fit was verified in each data trace by plotting the fitted eigenvector over the components of desaccaded eye velocity trajectories in two and three dimensions (Wearne et al. 1996, 1997a,b). In the text, single values are used when describing specific data traces to aid the reader in evaluating the figures. Whenever a data set was considered, means ± SD are given.

At the end of the experiments, animals were deeply anesthetized

and perfused intracardially with saline and 10% Formalin. The brains were removed, embedded in celloidin, and serially sectioned in sagittal stereotaxic planes. Sections were stained with cresyl violet, and the extent of the lesions was reconstructed. The atlas of Madigan and Carpenter (1971) was used as an aid in plotting the location of the lesions. Roman numerals were used to denote the uvula (IX) and nodulus (X) for clarity. In other contexts, the numerals 9 and 10 refer to the uvula and nodulus, respectively.

RESULTS

Description of nodulo-uvular lesions

Sagittal sections in *monkey M9312*, in whom the entire nodulus and most of the uvula were removed are shown in Fig. 2, *A* and *B*. The lesion was also reconstructed on sagittal sections from a normal rhesus cerebellum (Fig. 2*C*) (Madigan and Carpenter 1971). The sections, ~0.5, 2.5, and 3.75 mm to the left (*A*) and right (*B*) of the midline, correspond to Zones 1, 3, and 4 of Voogd et al. (1996) in the rhesus monkey. Medial portions of the nodulus and uvula were completely removed, and tissue was absent ventral to the secondary fissure (2°) [0.5 mm, Fig. 2, *A*, (1) *B*, (1) and *C*, Zone 1]. Laterally, the nodulus and uvula were completely ablated on the right (Fig. 2*B*, (3) R 2.5 mm; Fig. 2*C*, Zone 3, 2.5 mm), but a small portion of the dorsal uvula remained 2.5 mm from the midline on the left (Fig. 2*A*, (3), L 2.5 mm). The uvula was absent at 3.75 mm level, and the paramedian lobules (PML) were shifted toward the midline [Figs. 2*A*, (4) and *B*, (4), 3.75 mm]. Three other animals (*M1107*, *M1152*, and *M1153*) from an earlier study (Waespe et al. 1985) had similarly complete lesions (Table 1).

Partial lesions of the nodulus and uvula were made in *M9303* in the current study and in *M1173* and *M1175* in an earlier study (Cohen et al. 1992). In each case the lesions were confined to the vermal portions of the nodulus and uvula, and the lateral portions of the nodulus were intact. The lesion was symmetric in *M9303*. Sections of the lesion 0.5, 2.5, and 3.75 mm from the midline in *M9303* are drawn in Fig. 3, *A* and *B*, and the extent of the lesion was reconstructed on a normal cerebellum in Fig. 3*C*. The lesions in *M1173* and *M1175* are presented in Fig. 9 of Cohen et al. (1992), and a section is shown in Fig. 14*B*. In *M9303*, the central regions of lobules 9d and 10 of the caudal vermis were removed en bloc, extending to the lateral margins of the uvula [Fig. 3*A*, (1) *B*, (1) and *C*, Zone 1 (0.5 mm)]. The lateral-most 1.8 mm of the nodulus, corresponding to rhesus monkey zones 3 and 4 of Voogd et al. (1996), were left intact [Fig. 3, *A*–*C* (2.5 and 3.75 mm)]. Purkinje cells in this region had a normal appearance with intact nuclei and cytoplasm. Approximately 70% of the nodulus and rostral-ventral uvula (sublobule 9d) were destroyed in *M1173* and *M1175*, also leaving lateral portions of the nodulus intact.

The complete and partial lesions are compared in the schematic of Fig. 4, ad related to the histochemically defined zones of Voogd et al. (1996). All of the nodulus and lobules 9c and 9d of the uvula were ablated in the complete lesions, whereas all or most of Zone 1 and most of Zone 2 of the nodulus and lobules 9c and 9d of the uvula were ablated in the partial lesions. This left a margin of intact nodulus and ventral uvula in Zone 2 and all of Zones 3 and 4 in the partial animals.

Complete nodulo-uvulectomy and the time constants of velocity storage

Time constants of the velocity storage component of the aVOR are dependent on orientation of the head relative to gravity in normal monkeys, and the horizontal and vertical/roll components vary inversely. In each case, the time constants are maximal when animals are positioned so that the axis of the angular stimulus is coincident with the spatial vertical (Angelaki and Hess 1994a,b, 1995; Dai et al. 1991, 1992; Matsuo and Cohen 1984; Raphan and Cohen 1986, 1988). Thus horizontal OKAN time constants are maximal in the upright position and decline as a function of tilt angle with animals side down, prone or supine (Dai et al. 1991; Wearne et al. 1996, 1997b). Postrotatory vestibular horizontal time constants are similarly reduced in side-down positions (Angelaki and Hess 1994a, 1995; Benson 1974; Guedry 1974; Raphan et al. 1992; Waespe et al. 1985). In contrast, vertical and roll OKAN and vestibular time constants are maximal in side-down or prone and supine positions (Dai et al. 1992), whereas the pitch and roll OKAN time constants become short when monkeys are upright (Matsuo and Cohen 1984; Raphan and Cohen 1988). This implies that the time constants of the velocity storage component of the pitch and roll aVOR are also short in the upright position.

After nodulo-uvulectomy in *M9312*, central horizontal velocity storage time constants, determined from OKAN and from per- and postrotatory nystagmus during rotation at 60°/s with the animal in an upright position, increased on average from 12.0 s before to 23.6 s (Table 1; average of right and left values from Table 2). Horizontal aVOR time constants also increased on average from 29.3 to 59.2 s in the three other animals with complete nodulo-uvulectomy (Table 1). In contrast, vertical and roll time constants were short in every orientation after lesion (Fig. 5, *B* and *D*). On average, the aVOR vertical time constant for rotation about a spatially vertical axis fell in *M9312* from 10.1 to 3.5 s postoperatively, and the roll time constant from 13.4 to 2.7 s (Table 2). Vertical aVOR time constants fell on average in *M1107* and *M1152* from 18.0 to 5.9 s (Table 1). These effects were enduring and were present on repeated testing >1 yr after lesion.

The dependence of the OKAN time constants on gravity was also lost after nodulo-uvulectomy. Regardless of head position, the horizontal and vertical time constants remained close to those previously recorded in the upright position. The failure of reorientation of the head to affect the horizontal time constant after nodulo-uvulectomy has been demonstrated previously (Angelaki and Hess 1995; Waespe et al. 1985). The change in the sensitivity of the vertical time constant to gravity is shown in Fig. 6. Before lesion, *M9312* had strong upward OKN and OKAN in the left ear down position ($-\omega_X$; Fig. 6*A*), with an OKAN time constant of 13.3 s. Postoperatively, upward OKN was equally vigorous, but the on-side time constant of upward OKAN was now 2.5 s ($-\omega_X$; Fig. 6*B*). This is close to the mean upward OKAN time constant recorded in four cynomolgus monkeys when sitting erect (3.5 s) (see Fig. 6*A* of Dai et al. 1991).

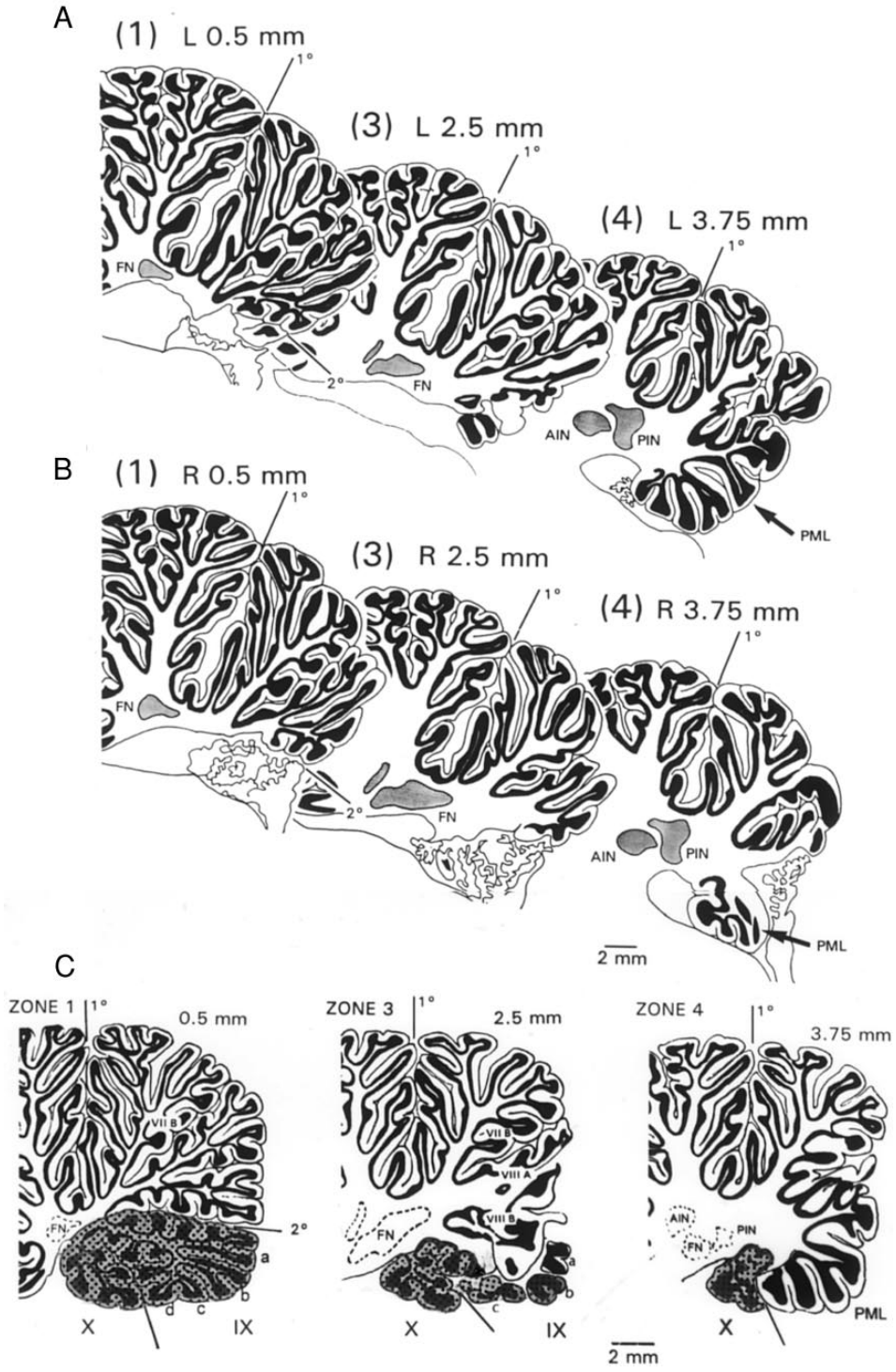

FIG. 2. Sagittal sections through the cerebellum in *M9312* in whom the nodulus and most of the uvula were removed. The drawings correspond to sections at ~0.5 mm, 2.5 mm, and 3.75 mm from the midline to the left (*A*) and right (*B*) of the midline. The numbers 1, 3, and 4 correspond to the rhesus monkey zones of Voogd et al. (1996). The arrows point to the paramedian lobule in the lateral-most sections. *C*: normal rhesus monkey sagittal sections (Madigan and Carpenter 1971) at 0.5 mm (Zone 1), 2.5 mm (Zone 3), and 3.75 mm (Zone 4) from the midline. The superimposed shaded regions indicate the extent of the lesion in *M9312*. Because the lesions were symmetric, only one side is shown in the reconstruction. FN, fastigial nucleus; AIN, anterior interposed nucleus; PIN, posterior interposed nucleus; PML, paramedian lobule. 1° and 2° refer to the primary and secondary fissures. IX and X refer to the nodulus and uvula, respectively. The uvula is further divided into sublobules a–d.

In conjunction with the increase in the horizontal time constant, each of the completely lesioned animals developed periodic alternating nystagmus (PAN; Table 1) (Waespe et al. 1985). The PAN was somewhat asymmetric in *M9312*, being shorter to the left than to the right, with a mean period of 170 s (Fig. 7). The velocity vector of the nystagmus was predominantly horizontal (ω_Z), but there was a small torsional component (ω_Y) that tipped the vector back in the head, as well as nonperiodic spontaneous downward nystagmus. Horizontal PAN was also present in each of the other three animals with complete lesions (Table 1). It developed spontaneously if animals were in darkness, but was also elicited by low-amplitude vestibular or optokinetic stimuli. The periods ranged from 150 to 250 s. PAN was suppressed in light. It disappeared with parenteral administration of small doses of baclofen (0.5–1 mg/kg) (Halmagyi et al. 1980), a γ-aminobutyric acid-B ($GABA_B$) agonist that shortens the dominant horizontal time constant of velocity

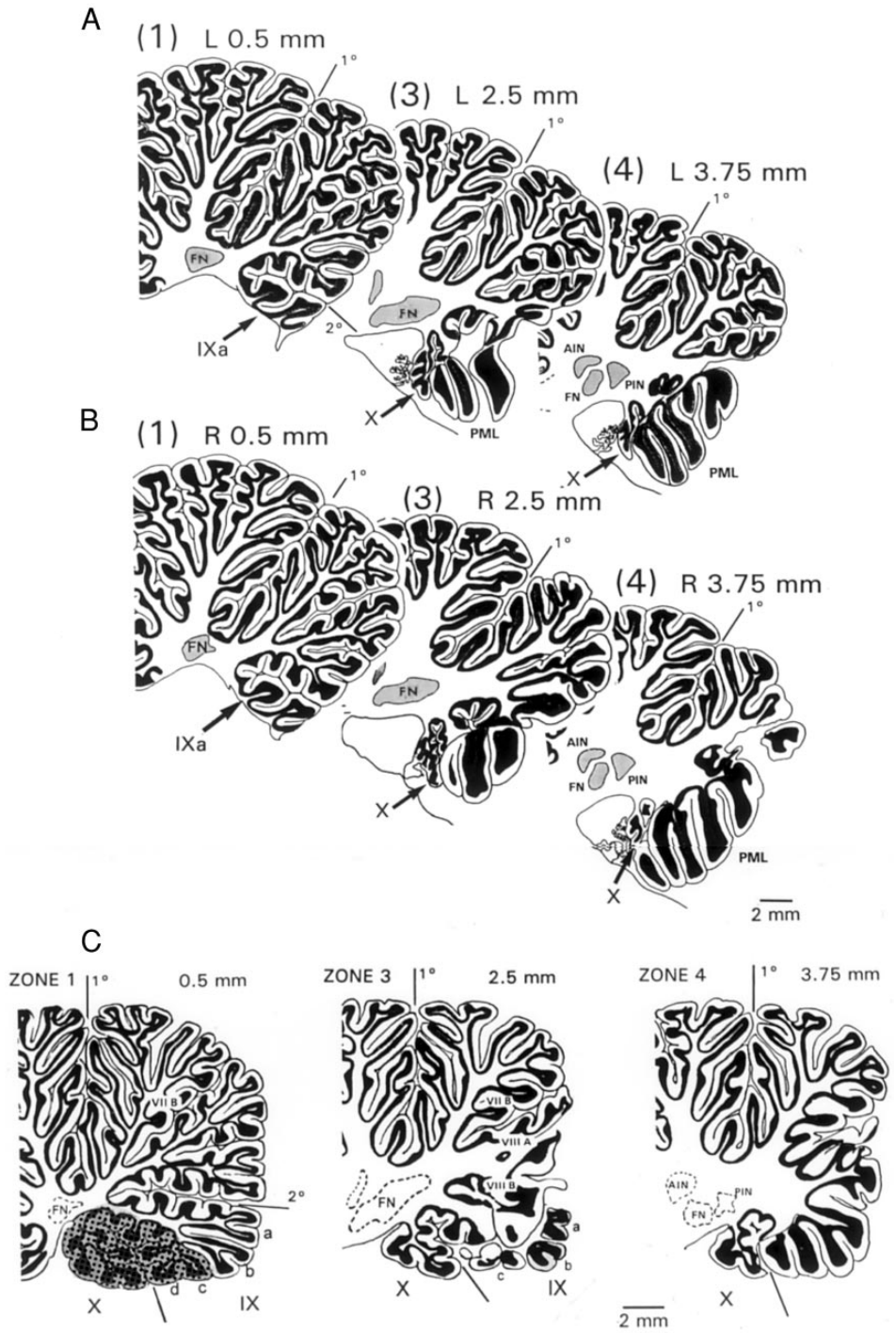

FIG. 3. Scheme as in Fig. 2. Sagittal sections through the partial lesion in *M9303*. Central portions of the nodulus and rostral-ventral uvula within 2 mm of the midline were removed. *A* and *B*: at 0.5 mm, only lobule 9a of the uvula was intact (arrows). At 2.5 and 3.5 mm, lateral portions of nodulus and lobule 9d of the uvula are visible. Arrows point to the residual nodulus. *C*: summary of the reconstruction showing the intact nodulus in Zones 3 and 4 (arrows).

storage (Cohen et al. 1987). This is consistent with the postulate of Leigh et al. (1981) that the oscillation of PAN is produced by large increases in the time constant of brain stem integrators, unchecked by inhibition.

Completely lesioned animals also lost the ability to reduce or ''dump'' horizontal slow-phase velocity during per- or postrotatory nystagmus and OKAN when they were exposed to a self-stationary visual surround (Waespe et al. 1985) (Table 1). In the example shown in Fig. 8*A*, horizontal eye velocity (ω_z) rapidly dropped by ~70% during the visual exposure, presumably due to activation of direct visual-oculomotor pathways that suppressed the nystagmus. Eye velocity returned to close to preexposure levels after the animal was once again in darkness and decayed with the same long time constant as the response in darkness. A small loss of stored velocity in Fig. 8*A* is expected, due to visual feedback from the eyes moving over the stationary surround during the period of suppression, rather than to activation of the dump mechanism (Waespe et al. 1985). Loss of control of the horizontal time constant in tilt- and light-dumping paradigms after nodulo-uvulectomy was present in each of the completely lesioned animals (Table 1).

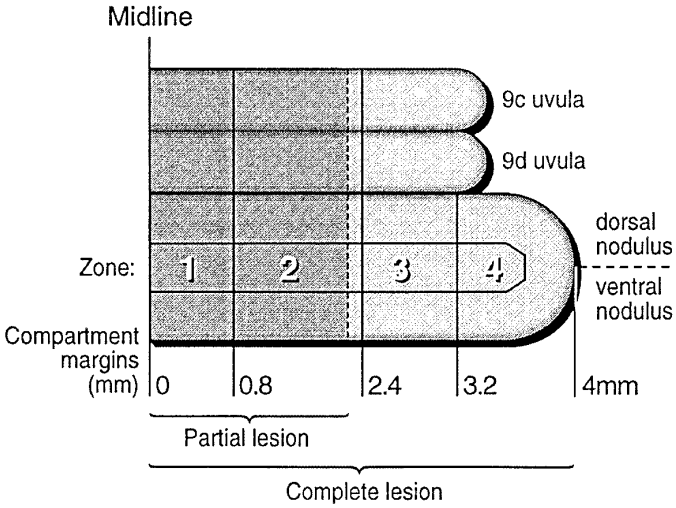

FIG. 4. Schematic diagram indicating complete and partial lesions of nodulus and uvula in the monkeys of this series, drawn on sagittal zones defined by Voogd et al. (1996) and J. Voogd (personal communication). Zones are based on AChE staining of margins of white matter compartments, which carry the climbing fibers to each zone. Numbers below represent mm from the midline.

Complete nodulo-uvulectomy and spatial orientation of the aVOR

During eccentric rotation (centrifugation) in the normal animal, the GIA vector tilts relative to the upright head. This has two consequences: the horizontal velocity storage time constant is reduced, and vertical cross-coupled components of eye velocity appear, tending to align the eye velocity axis with the GIA (Raphan et al. 1996; Wearne et al. 1996, 1997b). The completely lesioned animal lost both of these features. In the example shown in Fig. 9, the horizontal time constant for centered rotation was 13.5 s (Fig. 9*B*). Horizontal time constants for facing and back to motion centrifugation, which tilted the GIA by 51° about the nasooccipital axis, were the same whether facing motion (13.1 s, Fig. 9*A*) or back to motion (12.6 s, Fig. 9*C*). In addition, spatial orientation was lost, and there was no vertical (ω_X) or torsional (ω_Y) cross-coupling (Fig. 9, *A* and *C*). A small downward vertical component, present to the same extent during centered rotation (Fig. 9*B*, arrow A) as during facing and back to motion centrifugation (*B* and *C*), was probably spontaneous nystagmus. Ocular counter-rolling in response to the tilt of the GIA about the nasooccipital axis was preserved (Fig. 9, *A* and *C*; arrows B, ψ). It should be noted that the horizontal time constant was ~13 s in response to rotation at 400°/s during centered and off-center rotation (Fig. 9). This was substantially less than the average aVOR time constants of this animal when rotated at 60°/s (Table 2). The difference is due to the reduction in horizontal time constant as rotational velocity increases. This relationship originally described in normal animals (Raphan et al. 1979), was present after both partial (Cohen et al. 1992) and complete nodulo-uvulectomy. Thus it does not depend on the integrity of the nodulus and uvula.

Spatial orientation in the pitch plane was tested by radial centrifugation (facing nose in or out, Fig. 10). Before operation, a prominent cross-coupled roll component appeared during rotation, building to a peak after the angular acceleration had ended (ω_Y; Fig. 10*A*, arrowheads). In accordance with the backward tilt of the GIA, the roll component reversed during clockwise and counterclockwise rotation in the nose-out orientation. The time constant of the roll component was long and was approximately equal to the time constant of the horizontal component (ω_Z). A small vertical component (ω_X) was also present during acceleration. The peak horizontal eye velocity was 140°/s, less than would be expected given the acceleration and peak velocity of the stimulus. This lower value was likely due to the reduction in the horizontal time constant produced by the tilted GIA. After lesion, the peak horizontal eye velocity reached 200°/s. This higher peak velocity was consistent with the loss of sensitivity of the horizontal time constant to the tilted GIA (ω_Z; Fig. 10*C*). There was a transient increase in roll eye velocity during the angular acceleration, concurrent with activation of the semicircular canals, but it decayed to zero

TABLE 2. *Complete nodulo-uvulectomy (M9312); OKAN and aVOR time constants about a vertical axis*

	Preop Left (+*Z*)	Preop Right (−*Z*)	Postop Left (+*Z*)	Postop Right (−*Z*)
		Horizontal		
OKAN	11.3 ± 2.1	12.7 ± 1.8	24.7 ± 4.8	22.5 ± 6.1
aVOR	12.6 ± 2.1	11.2 ± 1.4	17.0 ± 3.8	25.7 ± 4.2
	Preop Down (+*X*)	Preop Up (−*X*)	Postop Down (+*X*)	Postop Up (−*X*)
		Vertical		
OKAN	3.5 ± 0.7	13.5 ± 0.6	0.3 ± 0.2	3.5 ± 1.0
aVOR	9.8 ± 1.6	10.4 ± 2.6	2.2 ± 1.4	4.7 ± 1.5
	Preop CCW (+*Y*)	Preop CW (−*Y*)	Postop CCW (+*Y*)	Postop CW (−*Y*)
		Roll (prone)		
OKAN	12.0	13.7	3.7	1.6
aVOR	14.0 ± 3.5	12.7 ± 2.7	4.0 ± 0.8	4.4 ± 1.8

Values are means ± SD and are expressed in s. OKAN and aVOR time constants taken during self or surround rotation at 60°/s about a spatial vertical axis for *M9312* before and after complete nodulo-uvulectomy. CW, clockwise; CCW, counterclockwise. Other abbreviations, see Table 1.

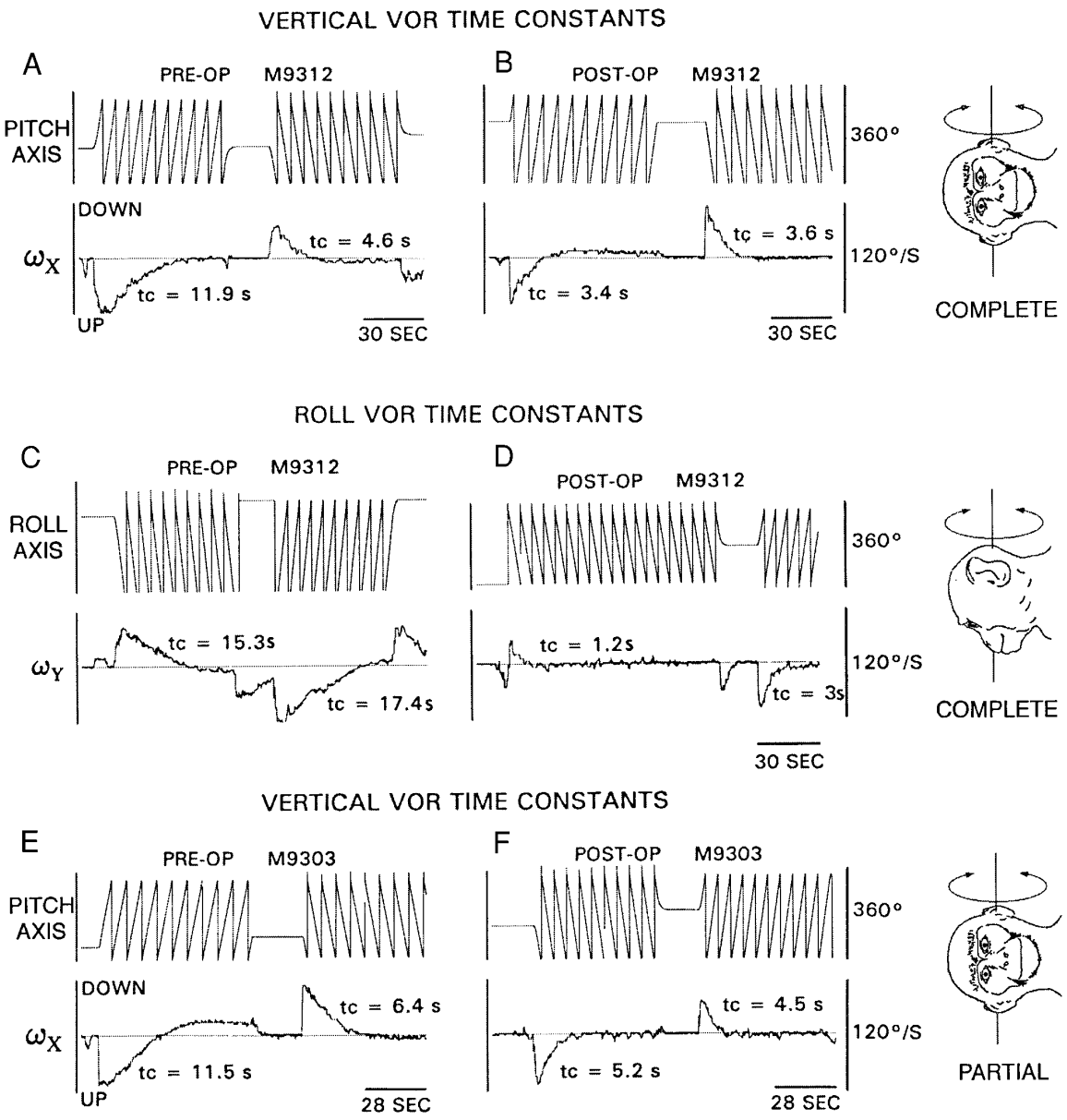

FIG. 5. Vertical (*A*, *B*, *E*, and *F*) and roll (*C* and *D*) angular vestibuloocular reflex (aVOR) time constants before and after complete (*A*–*D*) and partial (*E* and *F*) nodulectomy. As shown in the *insets*, animals were rotated left ear down or prone about a spatial vertical axis. *Top trace* in each part is yaw axis position, recorded with a potentiometer that resent every 360°. This gives the ''sawtooth'' appearance during constant velocity rotation. The *2nd trace* is desaccaded vertical (ω_X) or roll (ω_Y) eye velocity. The central (velocity storage) time constant is listed over each trace. It was obtained by a double exponential fit with the cupula time constant constrained to 4 s. Note the up-down asymmetry in the preoperative vertical eye velocity. Postoperatively, the time constants for upward and downward velocities were similarly short. The central time constant of roll after lesion fell to between 1 and 3 s.

when constant angular velocity was reached; in the constant angular velocity phase, there was no cross-coupling to roll.

The loss of spatial orientation is illustrated in the three-dimensional plots of the eye velocity trajectory representing a complete data set in this animal (Fig. 10, *B* and *D*). Preoperatively, the eye velocity axis tilted back in the head, aligning closely with the GIA for both directions of rotation. The fitted eigenvector (Fig. 10*B*, heavy line) is shown superimposed on the three-dimensional eye velocity trajectory (○). The components of the fitted eigenvectors for the $+\omega_Z$ and $-\omega_Z$ eye velocities to the right of the three-dimensional graph demonstrate the alignment of the eigenvector with the GIA. It tilted back in the head by 38° for $+\omega_Z$ eye velocities and 36° for $-\omega_Z$ eye velocities. This underestimated the 51° backward tilt of the GIA. Postoperatively, the eye velocity axis remained aligned with the *Z*-axis of the head (Fig. 10*D*, ○). The fitted eigenvector (heavy line) reflected this alignment. The *X* and *Y* components of the eigenvector were close to zero for both directions of rotation ($+\omega_Z$: *X*, −0.06; *Y*, 0.07; $-\omega_Z$: *X*, 0.02; *Y*, 0.01) and the *Z* component was close to 1 (0.99 and −0.99), producing negligible tilt of the eigenvector.

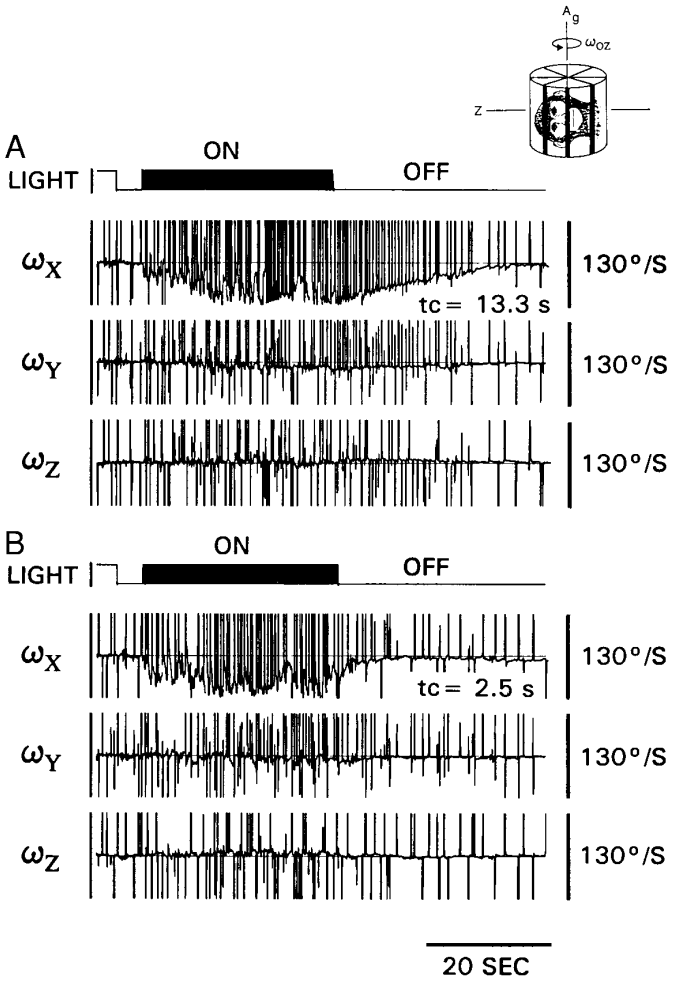

FIG. 6. Vertical optokinetic nystagmus (OKN) and OKAN before (*A*) and after (*B*) complete nodulo-uvulectomy. The animal was on its side, 90° right ear down (RED), and received upward optokinetic stimulation in pitch about a vertical axis (see *inset*). Preoperatively, there was strong upward OKAN, which decayed with a time constant of 13.3 s. Postoperatively, OKAN decayed rapidly with a time constant of 2.5 s.

Loss of axis reorientation for GIA tilts elicited in each cardinal head plane is shown in two-dimensional planar projections of eye velocity for tangential (Fig. 11*A*) and radial centrifugation (Fig. 11*B*). Before lesion, facing and back to motion (tangential) centrifugation induced roll-plane tilts of the eye velocity axis in the same direction as the GIA tilt (Fig. 11*A*, ■). Axis shifts in the roll plane were asymmetric, producing larger shifts during upward ($-X$) than downward ($+X$) cross-coupling. With right ear out, the axis tilted by 50 and 45° for upward and downward cross-coupling. With left ear out, it tilted by 32 and 25° for upward and downward coupling. Nose out in the radial orientation, the eye velocity axis tilted by 38° for $+\omega_Z$ and by 36° for $-\omega_Z$ eye velocities, and when nose in, by 70° for $+\omega_Z$ and by 34° for $-\omega_Z$ eye velocities (Fig. 10, *bottom row*, ■). After lesion (Fig. 11, ○), the eye velocity axis remained aligned with the head *Z*-axis during eccentric rotation, irrespective of the direction of GIA tilt, and there were only negligible tilts of the fitted eigenvector in both roll (*A*) and pitch (*B*) planes, similar to the alignment during centered rotation.

Thus complete nodulo-uvulectomy abolished axis reorientation of velocity storage associated with tilts of the GIA in any direction. This was true for all paradigms. Axis reorientation was not specifically tested with centrifugation in the other animals with complete nodulo-uvulectomy (*M1107*, *M1152*, and *M1153*), nor was ocular torsion measured. As noted, however, these animals had longer horizontal time constants and reduced vertical time constants after lesion, and their yaw axis time constants did not change when the animals were placed in positions that tilted the GIA with regard to the head during horizontal postrotatory nystagmus or OKAN (Waespe et al. 1985). This corroborates the loss of spatial orientation after complete nodulo-uvulectomy in these animals.

Partial nodulo-uvulectomy and time constants of velocity storage

After partial lesions that involved the central portions of the nodulus and uvula, animals retained control of the horizontal time constants, but lost control of the vertical and roll time constants. Thus the pitch and roll aVOR time constants were reduced for stimulation about a spatial vertical axis, as in the completely lesioned animals. Examples of reduction in the pitch aVOR time constant before and 1 wk after surgery are shown in Fig. 5, *E* and *F*; there was no recovery 4 mo later. The central (velocity storage) time constants of the vertical aVOR, recorded on-side in *M9303*, were reduced from 10.9 s to 1.7 ± 0.6 (SD) s for upward and from 8.6 s to 2.6 ± 0.4 s for downward slow phase velocities (Table 3). During velocity steps of 60°/s, either nose down (prone) or nose up (supine), the time constant of the roll VOR for both directions of rotation was reduced from an average 7.4 s before surgery to 2.2 s after surgery (Table 3).

In contrast, horizontal time constants were the same before and after partial lesions. Horizontal OKAN time constants were 14 s on average for leftward and rightward eye velocities in *M9303* before operation versus 15.5 s after operation (Fig. 12, Tilt angle 0°). The horizontal aVOR time constants

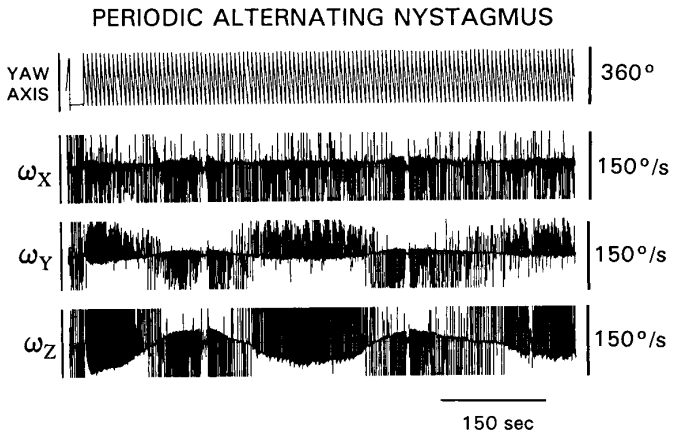

FIG. 7. Periodic alternating nystagms (PAN) following complete nodulo-uvulectomy in *M9312*. Nystagmus was initiated by a step of velocity of 60°/s in yaw around a yaw axis. Continuous oscillations developed in horizontal (ω_Z) and roll (ω_Y) eye velocity with a period of ~150 s. A sustained downward vertical nystagmus (ω_X) was also present.

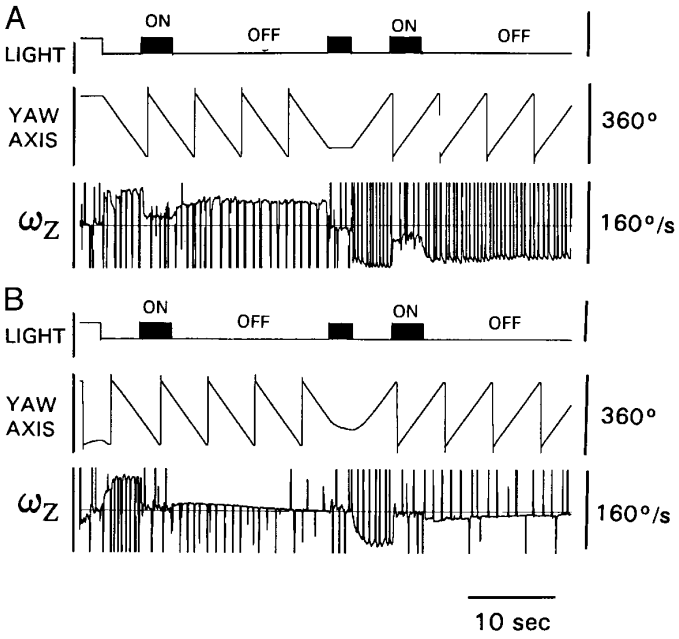

FIG. 8. Postoperative light-dumping in complete (*A; M9312*) and partially lesioned (*B; M9303*) animals during per-rotatory nystagmus. The animals and the surround were rotated at 60°/s in the same direction in darkness. The light was switched on (*top trace*, light on) for 4 s, exposing a self-stationary visual surround. There was little loss of stored eye velocity in the completely lesioned animal (*A*), whereas eye velocity had almost disappeared in the partially lesioned animal (*B*). Note the long horizontal time constant in the completely lesioned animal.

were 13.7 s in the first preoperative test and 12.5 s in the postoperative tests in this animal (Table 3). Similarly, the horizontal aVOR time constants were 26.5 s on average in the other partially lesioned animals before operation (*M1173* and *M1175*) and 24.0 s after operation (Table 1). None of the partially lesioned animals had periodic alternating nystagmus after surgery.

The ability to reduce the horizontal time constant when the GIA was tilted with respect to the head was quantified in *M9303* by measuring the horizontal OKAN time constant with the head tilted at angles of 0, 45, and 90° (Fig. 12). Before operation, the time constant for eye velocity to the right fell from 14.5 s at 0° to 9 s at 90°, with a slope of −0.09 s/deg of tilt (Fig. 12*A*). Postoperatively, the upright time constant was slightly longer (2.5 s), but the slope was the same (−0.1 s/deg vs. 0.09 s/deg). For leftward eye velocities (Fig. 12*B*), the preoperative slope was −0.06 s/deg. Postoperatively, the slope was slightly less (−0.03 s/deg). The ability to discharge velocity storage in response to rapid reorientation of the head during postrotatory nystagmus was also present in the other partially lesioned monkeys (Table 1).

All three animals with partial nodulo-uvulectomy were also able to discharge slow-phase eye velocity, i.e., to dump activity responsible for horizontal slow-phase eye velocity during conflicting visual stimuli (Table 1). Exposure to a self-stationary visual surround during steps of angular velocity in *M9303* produced a rapid drop in eye velocity and a loss of slow-phase velocity when the animal was once again back in darkness (Fig. 8*B*). In this instance, the 3.5-s period of suppression had resulted in an almost complete loss or dump of velocity storage. When the period of exposure was extended to 5 s, there was no nystagmus when the animal was once again in darkness. The ability of the partially lesioned animals to dump stored eye velocity as a result of exposure to a self-stationary visual surround is in contrast to the inability to discharge stored eye velocity in the completely lesioned animals under similar test conditions (Fig. 8*A;* Table 1).

Partial nodulo-uvulectomy and spatial orientation of the aVOR

Although partially lesioned animals maintained the ability to modify the horizontal time constant, they partially or completely lost the ability to orient the eye velocity axis to the tilted GIA. Thus, during centrifugation in *M9303* the predominant nystagmus velocity was horizontal (ω_Z) throughout stimulation, and there was no cross-coupling from yaw to vertical (Fig. 13, *A* and *C*; ω_Y, arrows A). Despite this, the horizontal time constant fell from 12.9 s when rotated on-center to 6.6 s when facing motion and 4.7 s when back to motion during centrifugation. Ocular counter-rolling was also normal after operation (Fig. 13, *A* and *C*; ψ, arrows B).

Spatial orientation was similarly affected during OKAN in *M1175*. The animal received yaw axis optokinetic stimulation at 60°/s for 30 s before the lights were extinguished and OKAN was recorded in darkness. Before lesion, peak values of vertical cross-coupled OKAN increased with side-down tilts, saturating at ~45°/s (46.4 ± 3.0°/s) with the animal tilted 70–120° on-side (Fig. 14*A*, ○). After partial nodulectomy (Cohen et al. 1992) (Fig. 14*B*), peak vertical cross-coupled OKAN was only ~11°/s (11.4 ± 1.8°) with the animal tilted in the same range (Fig. 14*A*, ●).

A complete data set from *M9303* during yaw axis OKAN was analyzed in two dimensions in all planes (Fig. 15), and eigenvectors were fitted to the three-dimensional data from the right ear down position (Fig. 16). Before operation, cross-coupling in *M9303* was robust. Upward coupling, i.e., cross-coupling from yaw to upward eye velocity, produced an 85° tilt of the fitted eigenvector in the roll plane with the right ear down, and downward cross-coupling a 58° tilt (Fig. 15*A*, ■, *left*; Fig. 16*A*). With the left ear down, upward coupling produced a 69° roll plane tilt, and downward coupling a 50° tilt (Fig. 15*A*, ■, *right*). Thus the animal demonstrated the same up-down asymmetry found in other normal monkeys when tilted in the roll plane (Dai et al. 1991; Matsuo and Cohen 1984; Matsuo et al. 1979; Wearne et al. 1997b). In the pitch plane, the fitted eigenvector tilted by 32° for $+\omega_Z$ and 38° for $-\omega_Z$ when nose down, and when nose up, it tilted by 77° for $+\omega_Z$ and by 66° for $-\omega_Z$ (Fig. 15*B*, ■). Postoperatively, cross-coupling was reduced but not abolished during GIA tilts in the roll plane. In the right ear down position, upward coupling produced a roll plane tilt of 39° and downward coupling a tilt of 16° (Fig. 15*A*, ○, *left*; Fig. 16*B*). For left ear down, upward coupling produced a tilt of 40° and downward coupling a tilt of 35° (Fig. 15*A*, ○, *right*). Three-dimensional analysis of this residual cross-coupling (Fig. 16*B*) demonstrated that both vertical and torsional cross-coupled components were present post-

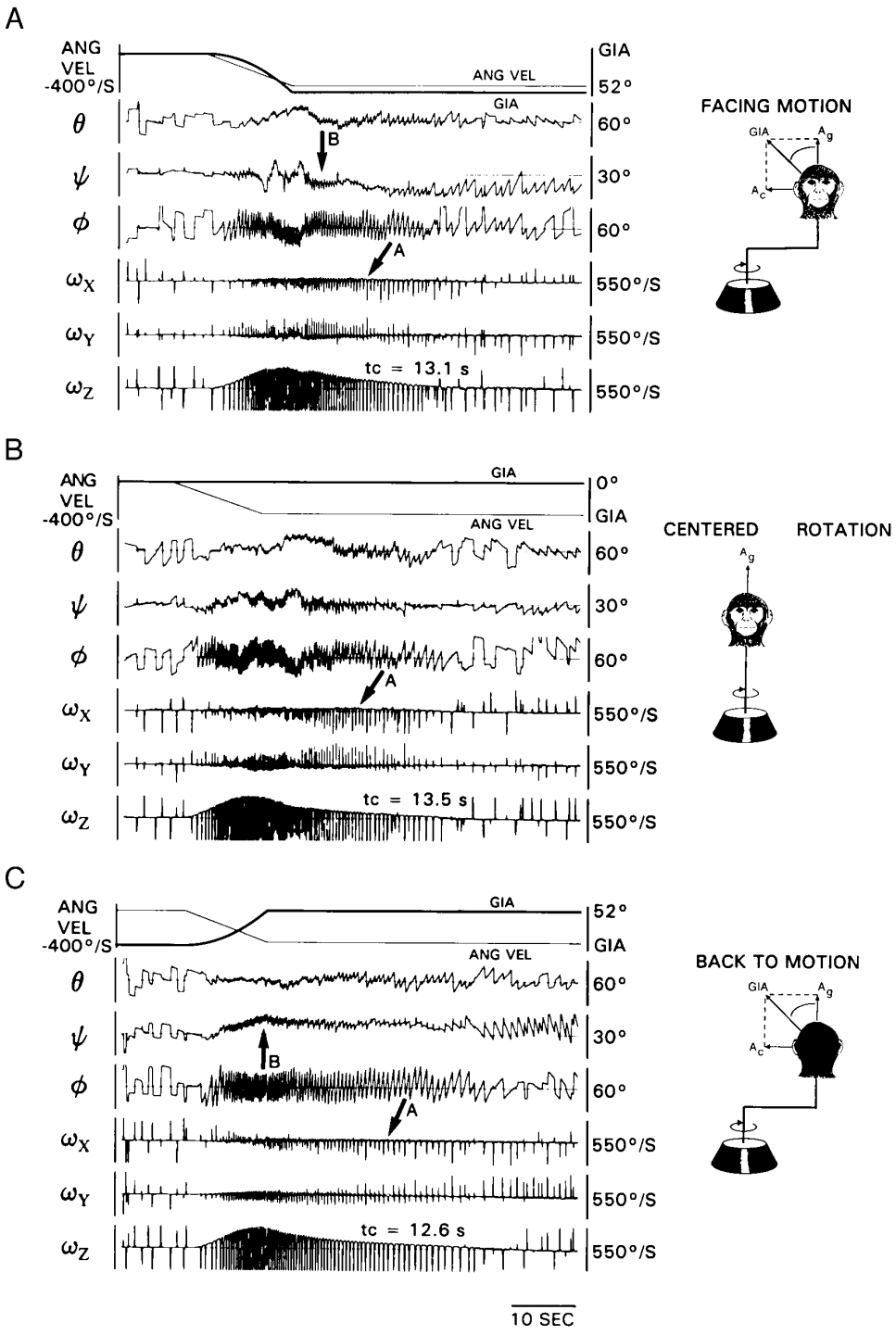

FIG. 9. Postoperative responses of *M9312* to $-Z$ yaw axis centrifugation. Eye position and eye velocity responses during centrifugation (*A* and *C*) and centered rotation (*B*) in yaw with an angular acceleration of 40°/s^2 up to a peak angular velocity of 400°/s. Three-dimensional eye position is represented using Euler angles in the Fick rotation convention, with (ϕ, θ, ψ) designating rotations about the yaw axis, the rotated pitch axis, and the optic (roll) axis in that order. Pitch (ω_X), roll (ω_Y), and yaw (ω_Z) components of the eye velocity vector are displayed in head coordinates. *Top panel* shows the angular and linear stimulus profiles over time: the angular velocity of the centrifuge (ANG VEL) is indicated with a light line and ranges from 0 to 400°/s; the corresponding tilt angle of the GIA is indicated with a heavier line. For centered rotation, the GIA tilt remains at 0°. *A–C*: time constant of horizontal eye velocity (ω_Z) was the same when facing or back to motion (*A* and *C*) as in centered rotation (*B*). Therefore it was unaffected by the tilted GIA. No cross-coupling from horizontal to vertical was present (compare arrows A in *A* and *C* with arrow A in *B*). During centrifugation, torsional eye position (ψ), shifted in the direction of the GIA tilt, indicating normal counter-rolling (arrows B).

operatively, but neither the magnitude nor direction correctly estimated the GIA tilt. Cross-coupling was abolished postoperatively for tilts in the pitch plane (Fig. 15*B*, ○).

Retention of control of the horizontal time constant and loss of control of cross-coupling was also demonstrated during reorientation of the head during postrotatory nystagmus (tilt-dumping). Per-rotatory horizontal time constants (ω_Z traces) were similar before and after lesion (15.1 s before, Fig. 17*A*; 14.2 s after, Fig. 17*B*) and fell rapidly when the head was reoriented both before [Fig. 17*A*, time constant (Tc) = 3.2 s] and after lesion (Fig. 17*B*, Tc = 4.3 s). Before lesion, a vertical component slowly developed with the head in the side down position ($-\omega_X$, arrow, Fig. 17*A*), shifting the axis of eye velocity by 90°, from alignment with the body yaw axis toward alignment with the spatial vertical axis. This is shown in the three-dimensional graph to the *right* of Fig. 17*A*. The fitted eigenvector (heavy line), computed as [−0.99, −0.05, −0.09], produced a roll plane tilt of 84.8°, which was close to the 90° tilt of the GIA. After lesion, cross-coupling during tilt dumping was lost. There

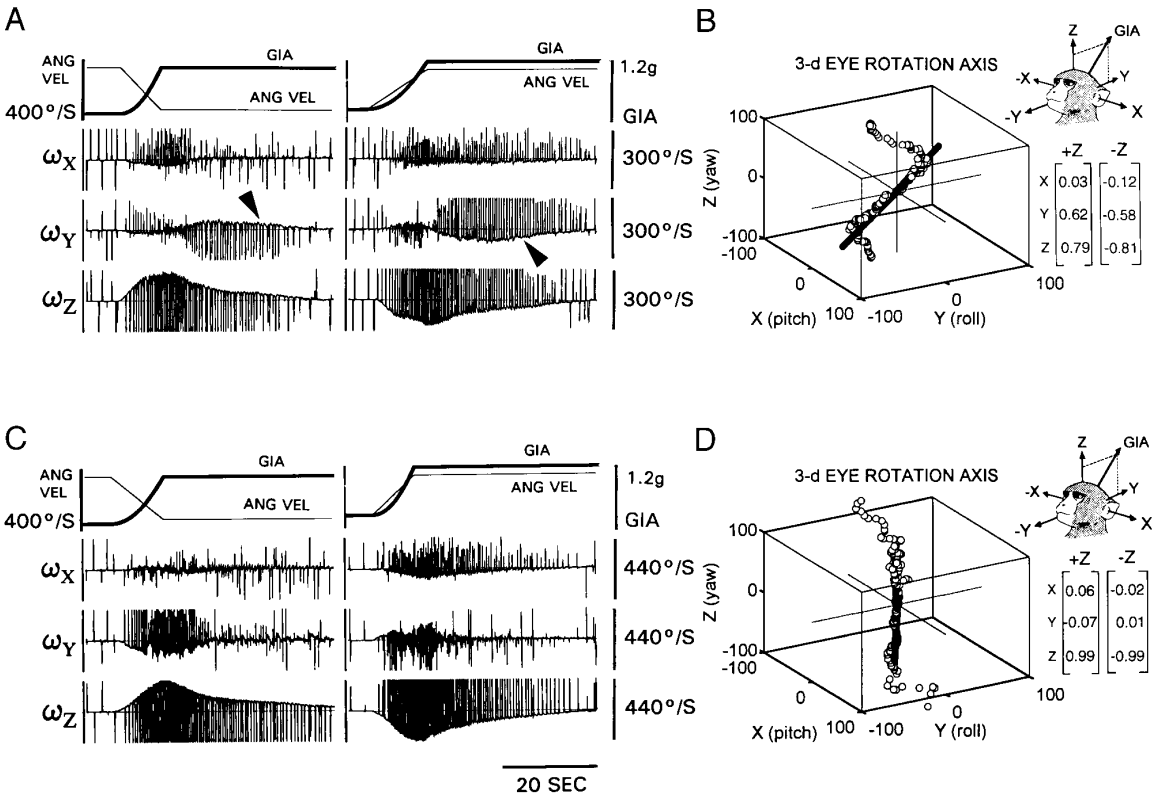

FIG. 10. Pre- (*A*) and postoperative (*B*) centrifugation in *M9312* in the radial orientation with the nose out. *A*: horizontal, vertical, and roll eye velocities for both directions of rotation. Centrifugation induced a positive cross-coupled roll component during $-Z$ rotation and a negative roll component during $+Z$ rotation (arrowheads). *B*: eye velocity axis plotted in 3 dimensions (○) with superimposed fitted eigenvector (heavy black line). Each graph is composed of 2 trials, one for $+Z$ and another for $-Z$ rotation. Circles start at the points farthest from the origin on the top and bottom halves of each graph and proceed toward zero. The eye rotation axis and the eigenvector both tilted back in the head by ~35–40°, slightly underestimating the tilt of the GIA (indicated on *inset* showing monkey's head). The components of the fitted eigenvectors for $+Z$ and $-Z$ horizontal eye velocity are shown in the *inset* to the far right of the 3-D graph. *C*: after nodulo-uvulectomy, eye velocity reached a higher peak due to the longer horizontal time constant. A roll component developed during angular acceleration in the direction opposite to that required to align the eye velocity with the GIA. This component decayed quickly and did not affect the final eye velocity trajectory. *D*: in 3 dimensions, the fitted eigenvector remained close to alignment with the *Z*-axis.

was a 7° tilt in both the pitch and roll planes (computed eigenvector [0.12, 0.12, 0.99]), but eye velocity remained closely aligned with the body yaw, not with the spatial vertical axis (Fig. 17*B*, heavy line, 3-D graph). Thus the reduction in cross-coupling for the population of partially lesioned animals in whom it was measured (*M1175* and *M9303*) was ≥80% in all orientations in all paradigms.

Model of control of spatial orientation

Neural implementation of spatial orientation of the aVOR was related to our general model of the aVOR and its extension to three dimensions (Raphan and Cohen 1996; Raphan et al. 1979; Raphan and Sturm 1991). The model, shown in Fig. 18, has a direct vestibular pathway with gain matrix, (G_1), which is independent of gravity (Wearne et al. 1997a). The nodulus and uvula do not control the direct pathway, but rather the parameters of velocity storage. While all central processing is performed in semicircular canal coordinates, the velocity storage system matrix, [H], has been transformed into head coordinates by the similarity transformation $[T_{can}^{-1}][H][T_{can}]$, where the matrix T_{can} represents the transformation from head ([X,Y,Z]) coordinates to semicircular canal coordinates, and T_{can}^{-1} the inverse transformation from canal to head coordinates (Robinson 1982; Yakushin et al. 1995).[3] In accordance with previous behavioral results (Dai et al. 1991), this structure shows that the time constants of horizontal, vertical, and roll are determined by the diagonal vertical elements. Cross-coupling, given by the nonzero off-diagonal terms, only occurs from horizontal to vertical and horizontal to roll. All other cross coupling terms are zero.

Insofar as zones identified on the basis of olivary input in the monkey have corresponding functions and efferent projections to those demonstrated in the rabbit, we suggest that the nodulus and ventral uvula could control spatial orientation of velocity storage in a canal-related coordinate frame by projecting from canal-related Purkinje cell zones to re-

[3]Showing the matrix in head coordinates simplifies the representation and demonstrates its upper triangular structure. This coordinate frame makes it clear which parameters of the system matrix are controlled by the various portions of the nodulus. In canal coordinates there would be no clear way to associate the parameters of velocity storage with the effects of partial and complete lesions.

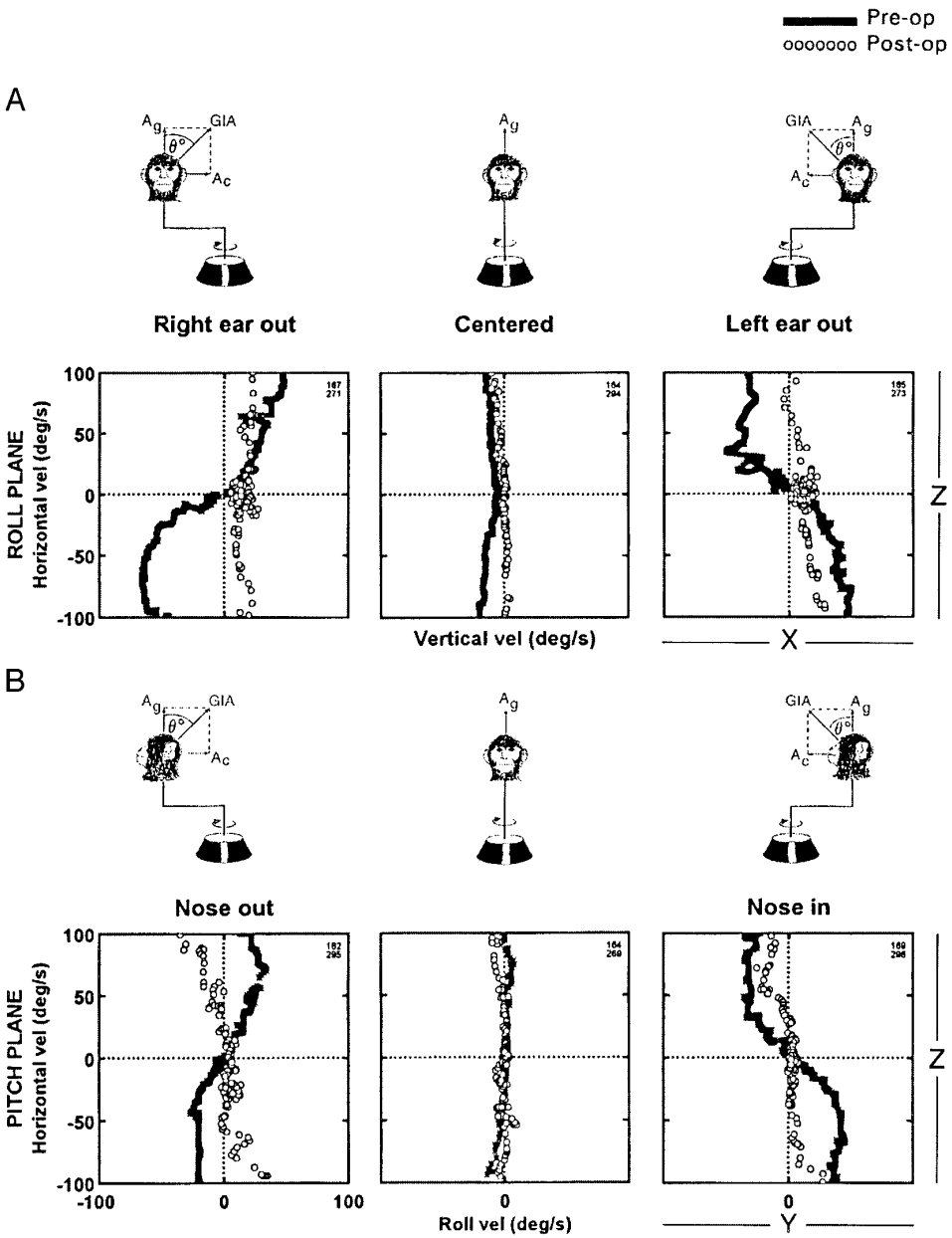

FIG. 11. Two-dimensional phase plane trajectories of eye rotation axes during centrifugation in *M9312*, which tilted the GIA by 52° in the roll (*A*) or pitch plane (*B*). Each graph is composed of 4 trials, one for $+Z$ and another for $-Z$ rotation before (■) and after operation (○). Circles start at the points farthest from the origin on the top and bottom halves of each graph and proceed toward zero. *A*: eye rotation axis during facing and back to motion centrifugation with right ear out (*left panel*), centered (*middle panel*), and left ear out (*right panel*). Preoperatively, the eye velocity axis gradually aligned with the GIA. Postoperatively, axis reorientation was abolished. *B*: eye rotation axis during centrifugation with nose out (*left panel*), centered, and nose in (*right panel*). Preoperatively, the axis tilted in the animal's pitch plane toward alignment with the GIA. Postoperatively, axis reorientation was abolished.

gions of peripheral superior vestibular nucleus (SVN) and rostral modial vestibular nucleus (MVN) containing canal-related vestibular-only (VO) and vestibular-pause-saccade (VPS) neurons (Fuchs and Kimm 1975; Reisine and Raphan 1992; Yokota et al. 1992). The aVOR integrator pathway, whose response characteristics are determined by the matrix *H*, is under parametric control by the nodulus and uvula, which adjusts the values of the time constants and the cross-coupled components. The arrows through the matrix entries indicate this. According to the results of this study, the vertical and roll time constants ($1/h_{11}$ and $1/h_{22}$) and cross-coupled components (h_{13} and h_{23}) are modulated by central portions of the nodulus and uvula (Zones 1 and 2), whereas lateral portions of the nodulus (Zone 3) control the horizontal time constant ($1/h_{33}$). Control of the horizontal time constant is independent of cross-coupling between axes. Because there is no cross-coupling from the pitch or roll to other axes (Dai et al. 1991; Raphan and Sturm 1991), activity responsible for cross-coupling flows from the yaw axis to the other axes, not the reverse.

Results of modeling responses before and after partial and complete nodulectomy

By altering the eigenvalues and cross-coupled components, the model simulated the responses in the normal, partially lesioned, and completely lesioned states during OKN and OKAN (Fig. 19). Simulations were performed in response to a surround velocity of 60°/s with the head upright and tilted 90° in side down and prone/supine positions. The stimulus states are shown by the *insets* on the side of Fig. 19, and correspond to each of the traces in that row. Normal responses are shown in the *first column*, and responses after partial and complete nodulo-uvulectomy in the *second* and *third columns*, respectively.

TABLE 3. *Partial nodulo-uvulectomy (M9303); aVOR time constants about a vertical axis*

	Preop Left (+*Z*)	Preop Right (−*Z*)	Postop Left (+*Z*)	Postop Right (−*Z*)
Horizontal	13.8 ± 1.3	13.7 ± 0.2	13.3 ± 1.2	11.7 ± 0.8
	Preop Down (+*X*)	Preop Up (−*X*)	Postop Down (+*X*)	Postop Up (−*X*)
Vertical	8.6	10.9	2.6	1.7 ± 0.6
	Preop CCW (+*Y*)	Preop CW (−*Y*)	Postop CCW (+*Y*)	Postop CW (−*Y*)
Roll (prone)	7.3 ± 1.5	7.4 ± 0.7	2.7 ± 0.9	2.9 ± 1.0
	Preop CCW (+*Y*)	Preop CW (−*Y*)	Postop CCW (+*Y*)	Postop CW (−*Y*)
Roll (supine)	N/A	N/A	1.6	1.5

Values are means ± SD and are expressed in s. aVOR time constants taken during angular rotation at 60°/s about a spatial vertical axis for partially lesioned monkey, *M9303.* Abbreviations, see Tables 1 and 2.

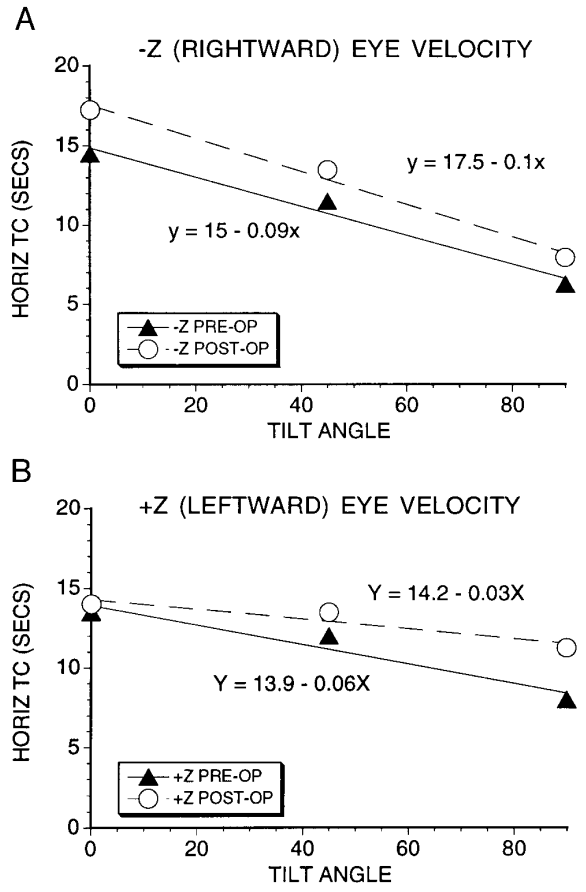

FIG. 12. Pre- and postoperative horizontal OKAN time constants in *M9303* as a function of head tilts, 0, 45, and 90° to LED and RED. Slope parameters were obtained from 1st-order linear regressions. Each data point is the average of 2 measurements. *A*: rightward OKAN eye velocities. Preoperatively (○), the time constant was ~14 s in the upright position, and fell with a slope of −0.09 s/deg. Postoperatively (▲), the upright time constant was several seconds longer, but the slope was not reduced by the partial lesion (−0.1 s/deg). *B*: leftward OKAN eye velocities. Preoperatively (▲), the slope was −0.6 s/deg. Postoperatively (○), the upright time constant was similar to preoperative values, whereas the slope (−0.03) was slightly reduced from the preoperative value.

To simulate the normal response in the upright position, the horizontal, pitch, and roll time constants were chosen as 12, 4, and 2 s, respectively (h_{11} = 0.25/s, h_{22} = 0.5/s, and h_{33} = 0.083/s; Table 2) with cross-coupling set to zero. For the normal response with the animal upright, the yaw component of OKN had a typical rapid and slow component, and the OKN and OKAN were purely horizontal. The OKAN had a time constant of 12 s (h_{33} = 0.0833) (Fig. 19*A*, Normal, Yaw). Pitch stimulation with the animal upright (Fig. 19*A*, Normal, Pitch) generated pure vertical OKN and OKAN of ~30°/s, which had a faster time constant (⩾4 s; h_{11} = 0.25/s). The normal roll response (Fig. 19*A*, Normal, Roll) induced pure torsional OKN and OKAN of ⩾20°/s, which had a time constant of 2 s (h_{22} = 0.5/s). There was no direct pathway response for roll OKN. After partial nodulectomy, these response characteristics were unaltered (Fig. 18*A*, *2nd column*, Partial).

Complete nodulectomy was simulated by setting the pitch time constant at 5 s, the roll time constant at 2 s, and the horizontal time constant at 50 s, and by removing cross-coupling (Fig. 19*A*, *3rd column*, Complete). This corresponded to the following parameter values for all head orientations: h_{11} = 0.25/s, h_{22} = 0.5/s, h_{33} = 0.02/s, h_{13} = 0, and h_{23} = 0. Complete nodulectomy did not alter the pitch or roll OKN or OKAN in the upright position. The increase in the horizontal time constant to 50 s resulted in a higher steady-state velocity of OKN and a much longer OKAN. The rising yaw time constant was shorter during OKN than the falling time constant during OKAN. This is due to visual feedback, which produces closed-loop behavior during OKN that is not much affected by even the large changes in the yaw time constant.

In side-down positions (Fig. 19*B*), the yaw-to-pitch cross-coupled parameter h_{13} was chosen to give an eigenvector of 10° relative to the spatial vertical (h_{13} = 0.02/s). During yaw OKN in the normal condition, this was associated with a shortened horizontal time constant (7.5 s; Fig. 19*B*, Normal, Yaw), and with the appearance of a cross-coupled vertical velocity that was not present in the upright condition (Fig. 19*B*, Normal, Yaw, arrow denoting pitch). The response to pitch stimulation was different from when upright (Fig. 19*B*, Normal, Pitch). Vertical OKN had a

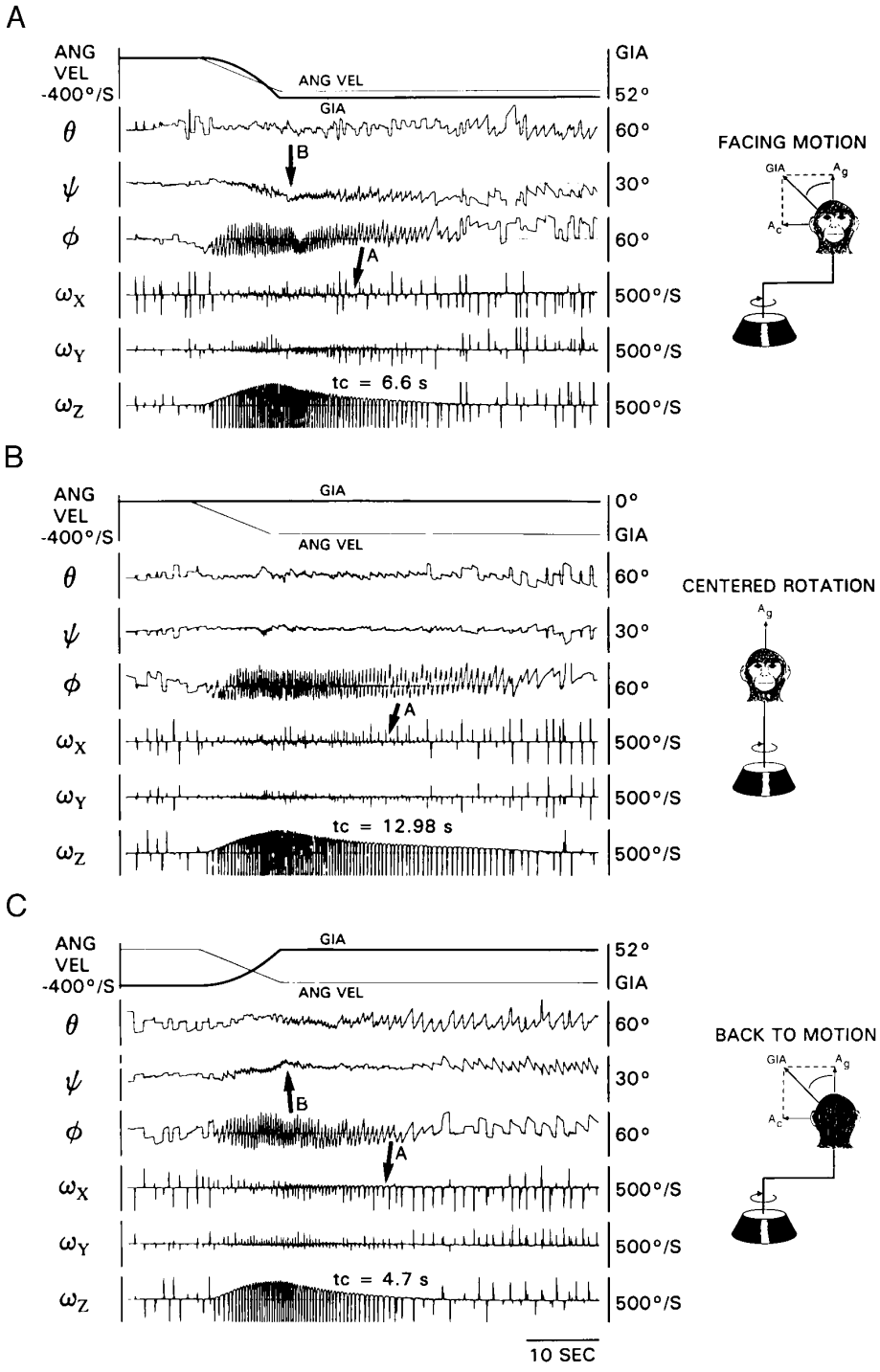

FIG. 13. Postoperative responses of *M9303* to $-Z$ yaw axis, facing (*A*) and back to motion (*C*) centrifugation and centered rotation (*B*) in yaw with angular acceleration of 40°/s^2 up to a peak angular velocity of 400°/s. Scheme as in Fig. 9. *A–C*: the time constant of horizontal eye velocity (ω_Z) was shorter when facing and back to motion (*A* and *C*) than when centered (*B*). Therefore sensitivity to the tilted GIA was unaffected from preoperative levels. No cross-coupling from horizontal to vertical was present (cf. arrow A in *A* and *C* with arrow A in *B*). During centrifugation, torsional eye position (*Y*) shifted in the direction of the GIA tilt, indicating normal counter-rolling (arrows B).

larger steady-state value (⩾40°/s), and the OKAN time constant was longer (T_c = 9 s; h_{11} = 0.11 s). The steady-state value and time constant of roll OKN and OKAN (not shown) were the same in the side-down and upright positions (Fig. 19*A*, Normal, Roll).

Partial nodulectomy reduced the gain of vertical OKN and the vertical OKAN time constant in the side down position in response to pitch stimulation (Fig. 19*B*, Partial, Pitch). Partial nodulectomy increased the horizontal OKAN time constant to 9 s (Fig. 19*B*, Partial, Yaw), but it was still smaller than when upright (12 s). Complete nodulectomy produced responses in the side-down condition that were identical to those in the upright condition (Fig. 19*B*, *3rd column*, Complete).

With the normal animal supine/prone receiving yaw stimulation, the yaw OKAN time constant was reduced to 7.5 s (Fig. 19*C*, Normal, Yaw), as for side-down positions, but the cross-coupling was to roll (Fig. 19*C*, Normal, Yaw, arrow denoting roll). The response to roll stimulation was different from when upright (Fig. 19*C*, Roll). The roll OKN had a larger steady-state value (⩾40°/s), and the OKAN time constant was longer (T_c = 9 s; h_{22} = 0.11 s). The

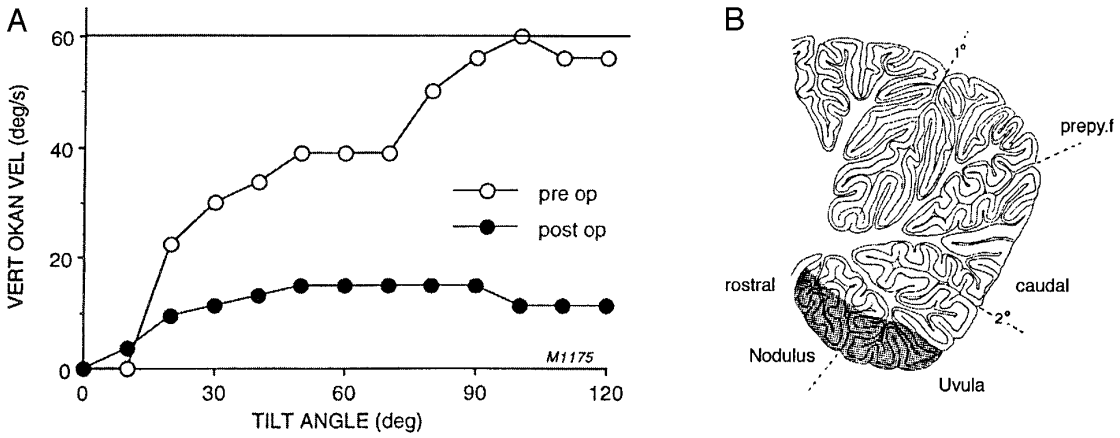

FIG. 14. *A*: maximal cross-coupled vertical (upward) velocities during yaw axis OKAN with animals tilted at various angles between 0° (upright) and 90° (on-side) in *M1175*, before (○) and after (●) the partial nodulo-uvulectomy shown in *B* (see Cohen et al. 1992, for a more complete description of lesion). Before lesion, peak vertical velocities were close to the velocity of stimulation (60°/s). After lesion, they fell to ~14°/s.

steady-state value and time constant of pitch OKN and OKAN (not shown) were unchanged from the upright condition (Fig. 19*A*, Normal, Pitch). Partial nodulectomy decreased the time constant of yaw OKAN to 9 s with the animal prone/supine (Fig. 19*C*, Partial, Yaw). The roll OKAN time constant, in response to roll stimulation, was unaltered from the upright condition and remained at 2 s (Fig. 19*C*, Partial, Roll). The yaw and roll time responses were unaffected in the prone/supine condition after complete nodulectomy and were similar to responses from the upright condition (Fig. 19*C*, Complete).

Thus, by modifying five parameters of velocity storage, the model developed from behavioral studies of OKN and OKAN (Dai et al. 1991; Raphan et al. 1992; Raphan and Sturm 1991) shows how the nodulus and uvula could control the spatial orientation and temporal aspects of the response to both optokinetic stimulation and centrifugation.

DISCUSSION

This study shows that by controlling the time constants and cross-coupling parameters of velocity storage, the nodulus and ventral uvula orient eye velocity toward the GIA. After removal of the nodulus and uvula, the horizontal aVOR and OKAN time constants were long, the vertical and roll time constants were short, and eye velocity induced by yaw axis stimulation remained fixed along the yaw axis of the head, irrespective of the manner in which the GIA tilt was induced. Thus the eye velocity vector was now independent of the direction of the GIA, and spatial orientation was fixed in a mode that corresponded to the upright position in a gravitational field.

Spatial orientation of the aVOR has been modeled by three independent processes: control of the horizontal time constant, control of the vertical and roll time constants, and generation of cross-coupled vertical and roll velocity components as the GIA tilts relative to the head (Dai et al. 1991; Raphan et al. 1992, 1996; Raphan and Sturm 1991; Wearne et al. 1996, 1997a,b). A fundamental finding of this study was that complete lesions resulted in an inability to modulate both the horizontal and vertical time constants, but that control of the horizontal time constant was retained in each of the animals with partial lesions. This is sufficient to show that parts of the nodulus that were left in the partial animals were responsible for control of the horizontal time constant. It also strongly suggests that the parts of the nodulus that were removed in the partial *animal M9303* were responsible for the loss of control of the vertical time constant. This was supported by findings in both *M1173* and *M1175*, in which yaw to vertical cross-coupling was greatly diminished. From this, we hypothesize that the function of medial regions of the nodulus (Zones 1 and 2) and ventral uvula is related to control of vertical and torsional time constants and to cross-coupling. These regions produce gravitational dependence of vertical and roll time constants when animals are in side-down or supine/prone positions, and adjust these time constants when the GIA tilts with regard to the head. In contrast, lateral portions of the nodulus (Zone 3) appear to exert tonic control of the horizontal aVOR time constant and mediate its dependence on relative tilts of the GIA.

Angelaki and Hess (1994a, 1995) have also implicated the nodulus and ventral uvula in the control of spatial orientation. They found a similar reduction of orientation to the GIA after nodulo-uvulectomy, but dynamic control of time constants was lost only for torsional eye velocities. From this, they inferred that the nodulus and uvula predominantly control roll eye velocity. In our study, however, vertical and roll time constants were concurrently reduced for vestibular and optokinetic stimulation whenever the nodulus and uvula were damaged (Figs. 5 and 6; Tables 1–3). There was some residual vertical cross-coupling during OKAN in tilted positions in *M9303* (Figs. 15*A* and 16*B*). However, the three-dimensional plots show that the magnitude of the cross-coupled components was inappropriate postoperatively, and an additional orthogonal component was present that caused misalignment of the eye velocity axis with the GIA. Moreover, vertical and torsional cross-coupled components were lost in this animal during facing and back-to-motion centrifugation (Fig. 13), during OKAN with the animal prone or supine (Figs. 14 and 15*B*), and during rapid reorientation

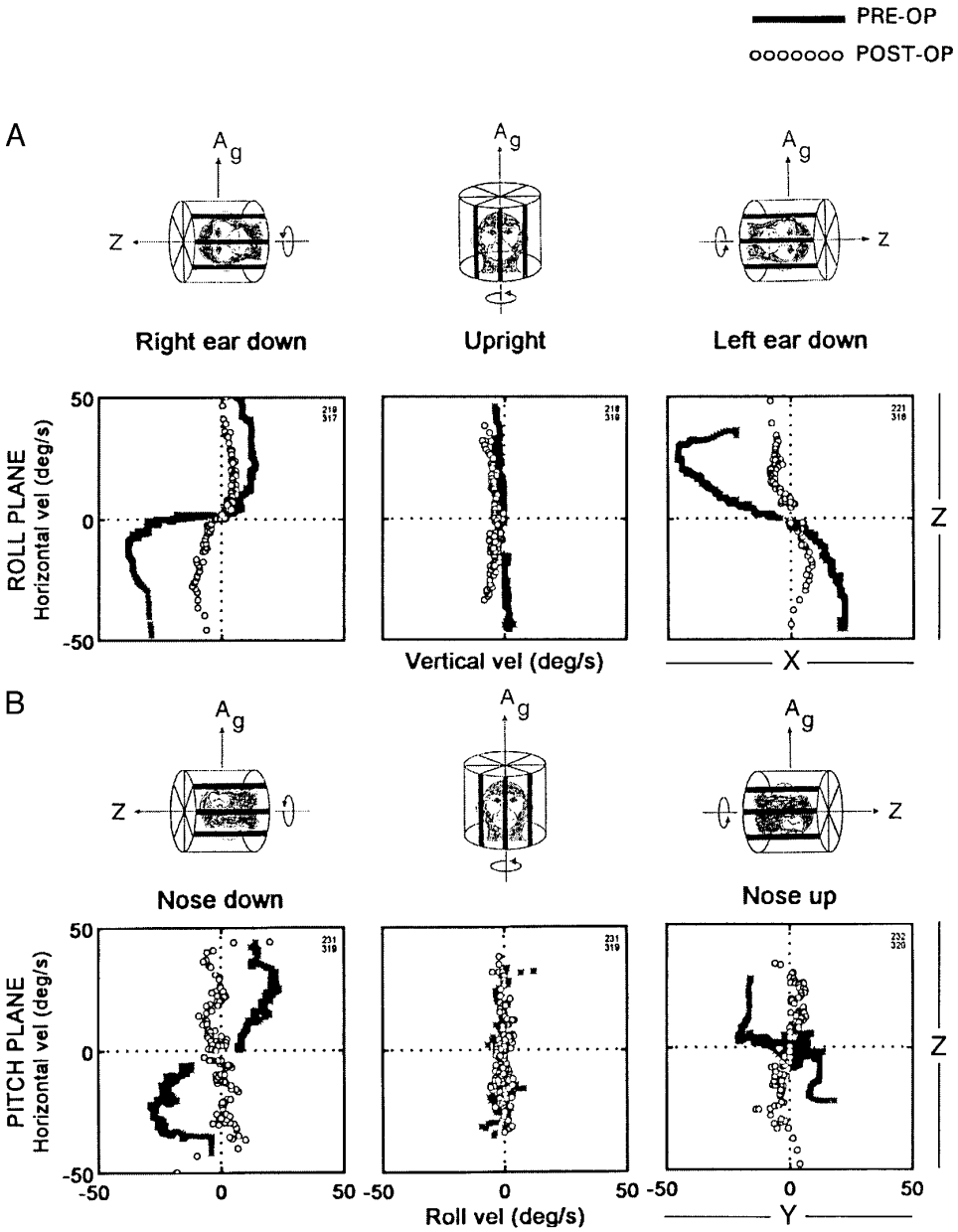

FIG. 15. Two-dimensional phase plane trajectories of eye rotation axes during OKAN in *M9303* with the head tilted the GIA left and right ear down (*A*) or prone and supine (*B*). Scheme as in Fig. 11. Preoperatively (■), the eye rotation axis was tilted more for upward than for downward cross-coupled components. Postoperatively, cross-coupling was markedly reduced but not abolished in the roll plane (*A*). *B*: preoperatively, the eye rotation axis tended to align with the GIA when the animal was supine (■, *right panel*), but tilted by less than ½ the angle when the animal was prone (■, *left panel*). Postoperatively, axis reorientation was abolished in the pitch plane.

in the roll plane during postrotatory nystagmus (Fig. 17). Presumably, the residual cross-coupling was produced by portions of Zone 2 of the nodulus that remained in *M9303* (Fig. 4). A similar explanation may account for the discrepancy between the two studies, i.e., the differences may be related to differences in portions of the nodulus or uvula that were ablated or spared.

It should be noted that the short vertical and roll time constants were not due to a loss of velocity storage. Had velocity storage been abolished, no OKAN would be present, as after bilateral labyrinthectomy (Uemura and Cohen 1973) or midline section (Katz et al. 1991; Wearne et al. 1997a). Rather, the vertical and roll time constants (≈2.5 s) were characteristic of the vertical and roll time OKAN time constants in the upright animal (Dai et al. 1991). It is not possible to measure vertical and torsional VOR time constants with animals upright and rotating about a horizontal axis, because this induces concurrent otolith activation that also produces eye velocity. However, aVOR and OKAN time constants measure activation of the same velocity storage mechanism (Raphan et al. 1979), and on-side vertical aVOR time constants were consistent with the on-side and upright vertical OKAN time constants (Table 2). Examples of short on-side vertical time constants, similar to those recorded in the upright position, are shown in Figs. 5 and 6*B*.

A longitudinal organization in semicircular canal-related Purkinje cell zones have been demonstrated in the nodulus and flocculus of a variety of species. Cerebellar modules, each comprising a Purkinje cell zone, its olivocortical afferents and corticonuclear efferents, have been proposed as basic functional computing units in cerebellar control of individual motor subsystems (Ito 1984; Oscarsson 1969, 1979; Voogd and Bigaré 1980; Voogd et al. 1996). This modular organization suggests a physical basis for the separate con-

trol of horizontal and vertical/roll time constants and cross-coupling parameters found in this study. In rabbit, Wylie et al. (1994) have correlated the climbing fiber zones of the ventral surface of the nodulus with Purkinje cell projections to the vestibular and deep cerebellar nuclei. In this and other species, nodular Purkinje cells target peripheral regions of SVN (Angaut and Brodal 1967; Haines 1977; Wylie et al. 1994), caudal MVN (Brodal and Brodal 1985; Haines 1977; Shojaku et al. 1987; Walberg and Dietrichs 1988; Wylie et al. 1994), and rostral MVN (Haines 1977; R. McCrea 1995, personal communication). Neurons that are believed responsible for the production of velocity storage are located in the targeted portions of peripheral SVN and rostral MVN (Holstein et al. 1996; Reisine and Raphan 1992; Yokota et al. 1992). On the basis of the results of our study, we suggest that parameters of velocity storage are controlled by the specific projections from separate zones in the nodulus to these neurons in SVN and MVN. More specifically, projections from the medial Zones 1 and 2 in the nodulus to SVN could control the vertical and torsional components of the cross-coupled responses and the vertical and roll time constants, whereas projections from lateral Zone 3 to MVN could control the horizontal (yaw) time constant.

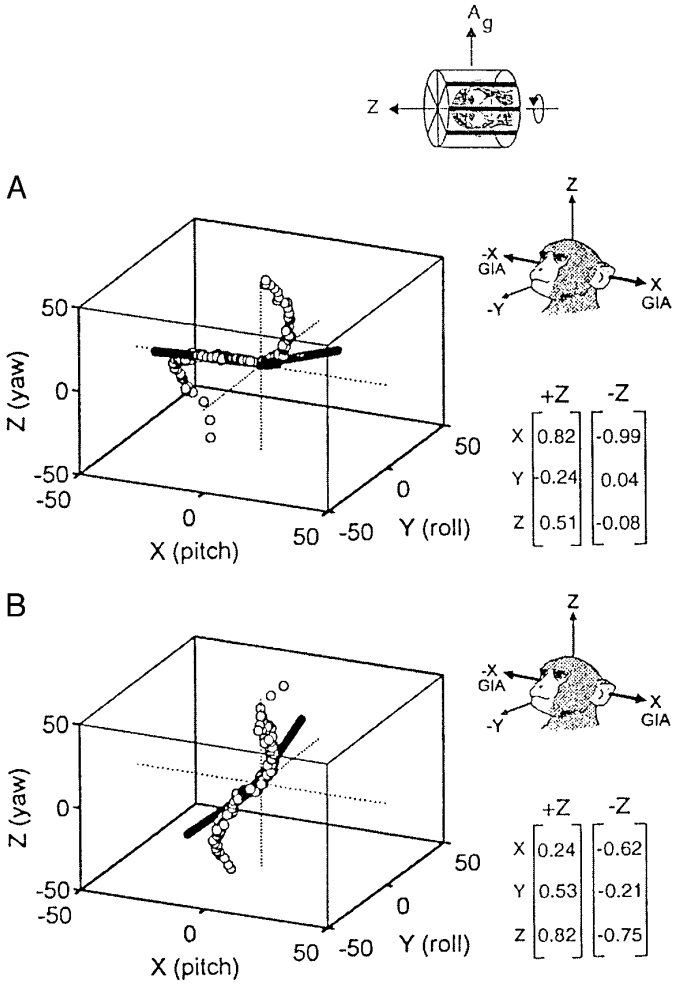

FIG. 16. Pre- (*A*) and postoperative (*B*) OKAN with head tilted right ear down in partially lesioned monkey *M9303*. The axis of eye velocity is plotted in 3 dimensions (○) with superimposed fitted eigenvector (heavy black line). Scheme as in Fig. 11*B*. *A*: for $+Z$ eye velocity, a downward cross-coupled vertical component appeared that tilted the eye rotation axis and the fitted eigenvector by 58° in the roll plane. For $-Z$ eye velocity, a stronger upward cross-coupled component was present, tilting the eye velocity and fitted eigenvector by 85.3° in the roll plane. *B*: after operation, cross-coupling in both directions was reduced, and the fitted eigenvector was no longer confined to the animal's roll plane. For $+Z$ eye velocities, the fitted eigenvector tilted by 16.3° in the roll plane and by 32.8° in the pitch plane. For $-Z$ eye velocities, the eigenvector tilted by 39.6° in the roll plane and by 15.6° in the pitch plane.

In a previous study (Cohen et al. 1992), the partially lesioned animals, *M1173* and *M1175*, lost all previous habituation of the horizontal time constant as well as the ability to habituate the horizontal time constant further on repeated rotational stimulation after medial lesions. This suggests that the medial nodulus may also have some function related to control of the horizontal time constant. Consistent with this, there is input from the caudal dorsal cap [VA (Yaw) OKN] to Zone 1 in the nodulus in the rabbit (Wylie et al. 1994), and electrical stimulation of central portions of the nodulus and uvula in the monkey shortened the horizontal time constant (Solomon and Cohen 1994). One possibility is that gravitational and plastic (habituative) control of the horizontal aVOR time constants may be organized separately, with dependence of the horizontal time constant on gravity being mediated in lateral portions of the nodulus and plastic control of the horizontal time constant (habituation) being dependent on medial or medial plus lateral portions of the nodulus and uvula. There are other aspects of orientation that are not directly linked to control of velocity storage, which may also depend on the nodulus and uvula. Control of autonomic function, for example, appears to be mediated by the lateral zones of the nodulus that project to caudal MVN (Precht et al. 1976; Wylie et al. 1994; Yates 1992; Yates et al. 1993). The close relation between spatial orientation and nausea could be realized through the lateral nodulus, thereby providing a link between disorientation and motion sickness.

Anatomic and physiological studies suggest that lobule 9d of the uvula may also be involved in spatial orientation. Both the nodulus and lobule 9d of the uvula in the cat and rabbit receive similar primary vestibular input (Barmack et al. 1993a; Brodal and Hoivik 1964), and this input is likely to exist in the monkey. Both the nodulus and sublobule 9d have extensive interconnection with the vestibular nuclei, and with regions of the inferior olives that process optokinetic and vestibular information (Voogd et al. 1996). This is in contrast to sublobules 9a–c of the uvula, which have different anatomic connections and are likely to have different functions. For example, stimulation of sublobule 9d generated slow changes in eye velocity that long outlasted the stimulus (Heinen et al. 1992; Heinen and Keller 1996). In addition, postrotatory and OKAN time constants were shortened by stimulation of 9d in a manner similar to the changes produced by stimulation of the nodulus (lobule 10) and to the effects of tilt and light dumping (Solomon and Cohen 1994). In sublobules 9a–c, on the other hand, only rapid changes in eye velocity were induced by electrical stimulation, and storage was unaffected by stimulation or lesions (Heinen et al. 1992; Heinen and Keller 1996; Solo-

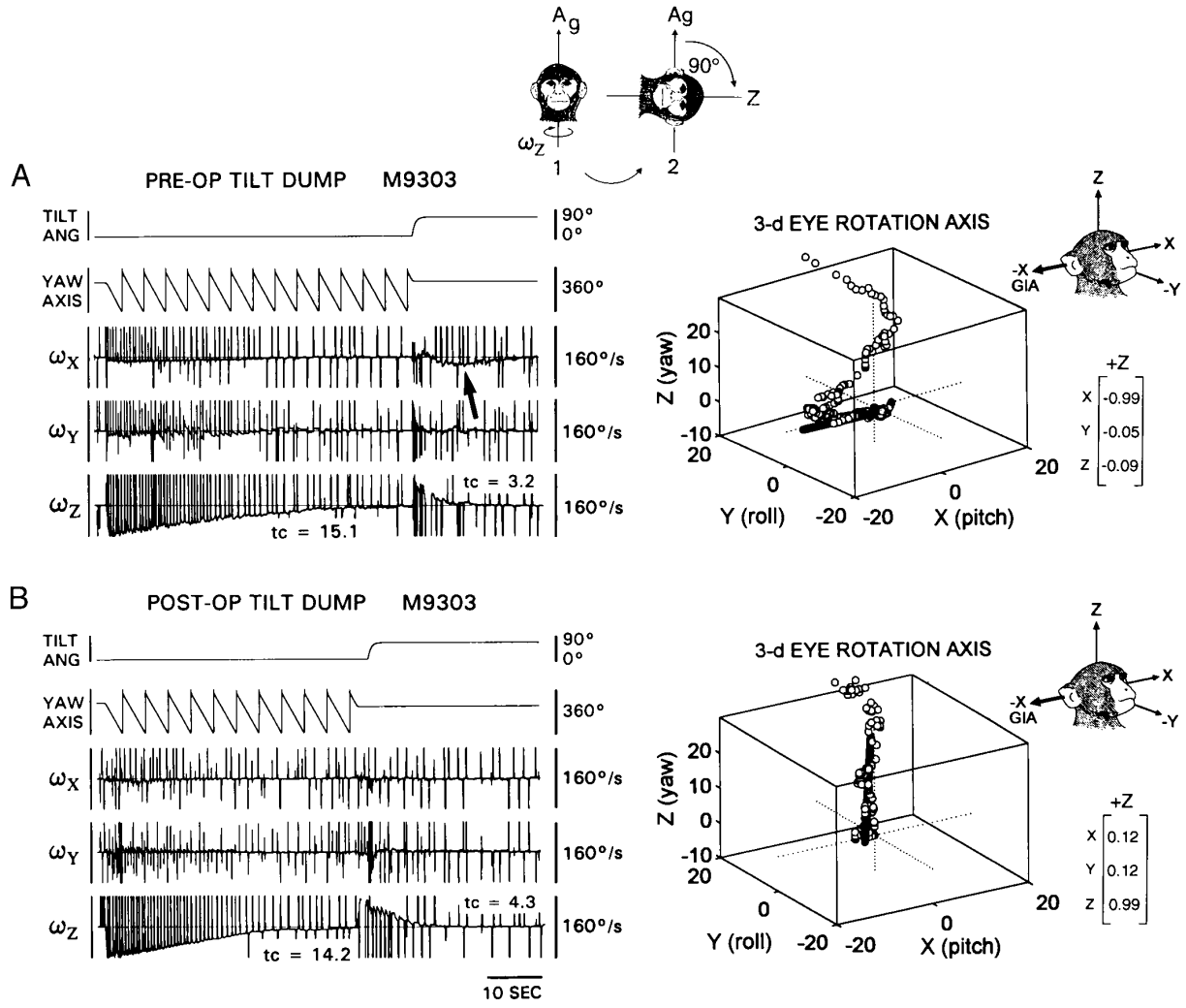

FIG. 17. Pre- (*A*) and postoperative (*B*) tilt dumping to left ear down (*top inset*) in partially lesioned *monkey M9303*. The direction of the GIA with the head tilted is represented by the arrow out of the right ear (*top right inset*). *A*: preoperatively the horizontal time constant was reduced (dumped) to 3.2 s as a result of head reorientation, and an upward cross-coupled vertical component appeared (arrow). The eye velocity trajectory is plotted in 3 dimensions in the graph on the *right.* The fitted eigenvector (black line) tilted by 84.8°, approximately aligning with the tilted GIA (*inset*). The eigenvector components, to the far right of the 3-D graph, reflect this tilt. *B*: postoperatively, the tilt dump following head reorientation was retained [time constant (T_c) = 4.3 s], but cross-coupling to vertical was lost (trace ω_X). As a result, the eye velocity axis and fitted eigenvector remained aligned with the head *Z*-axis (3-D graph on *right*, and eigenvector components).

mon and Cohen 1994;). Taken together, it is likely that the nodulus and sublobule 9d of the uvula comprise a functional unit that is related to control of velocity storage and its spatial orientation.

Different amounts of sublobules 9a and 9b of the uvula were removed in the partially and completely lesioned animals, and we considered whether they might have contributed to the behavioral results. On analysis, there was no apparent relationship between the extent of damage to sublobules 9a and 9b of the uvula and the components of spatial orientation. In a control animal, a lesion restricted to lobules 9a and 9b of the uvula did not affect control of either the horizontal or vertical time constants of velocity storage (Cohen, unpublished results). No lesion experiments have directly addressed the function of 9c, but the input and output projections of sublobule 9c (Brodal and Hoivik 1964) and the results of electric stimulation (Heinen et al. 1992; Solomon and Cohen 1994) suggest that it also is not functionally related to the nodulus and sublobule 9d.

To control spatial orientation of the aVOR, the nodulus and uvula must receive input from the otoliths about the GIA. An important question is how the orientation information from the otoliths, which have a wide distribution of polarization angles, is mapped onto the canal coordinates of the longitudinal zones. Climbing fiber input from the inferior olives related to the otoliths is localized to the most lateral zone of the ventral lamella and the central 0.5 mm of the nodulus in rabbit (Barmack et al. 1993a). This limited distribution and the low firing rates of climbing fibers make it unlikely that they could mediate the information required for spatial orientation. On the other hand, primary otolith afferent input that comes through mossy fibers is widely

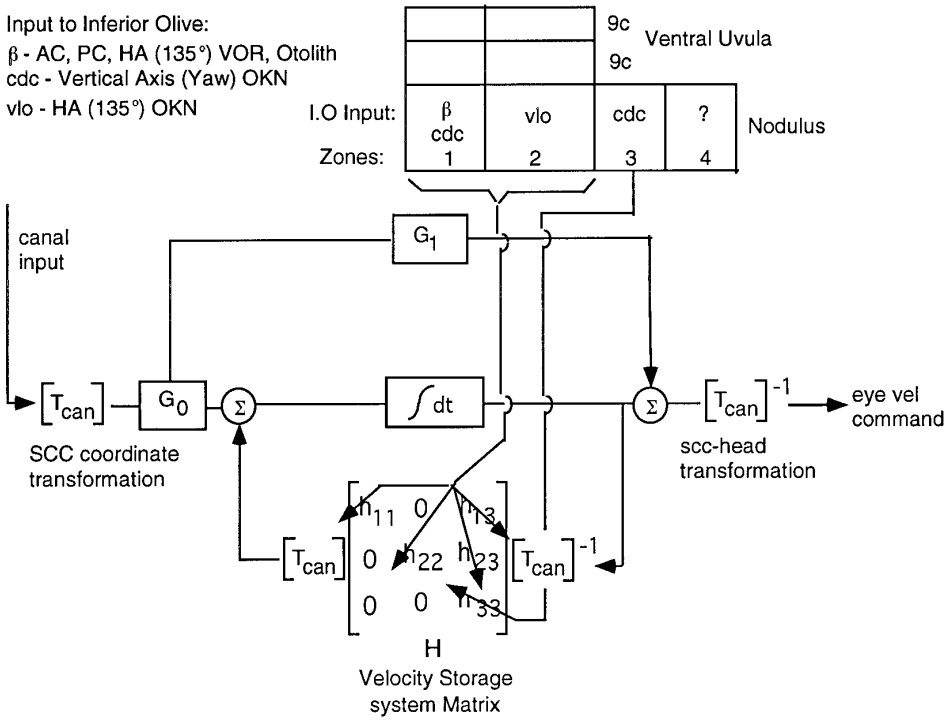

FIG. 18. Model of 3-dimensional control of orientation and dynamics of velocity storage system by the canal related zones of the nodulus and ventral uvula. Above are shown the 4 zones of the rhesus monkey nodulus, based on inferior olive input (Voogd et al. 1996). Zone 1 receives input from the β nucleus and the caudal dorsal cap (cdc). Zone 2 receives input from the ventrolateral outgrowth (vlo), and Zone 3 from cdc. Inputs to Zone 4 are still unidentified in the monkey. The inputs to the various subnuclei of the inferior olive are shown above and on left. G_0, gain matrix in integrator pathway; G_1, direct vestibular pathway gain matrix; T_{can}, matrix of head to canal coordinate transformation. See text for details.

distributed via granule cells through parallel fibers across the folia of the nodulus and lobule 9d (Barmack et al. 1993a; Brodal and Hoivik 1964; Marini et al. 1975), and there is direct input to mossy fibers from the vestibular nuclei. Mossy fibers have a patchy distribution (Bower and Woolston 1983), but they extend across several zones. Thus the critical information relating head position to the GIA is probably mediated by mossy fibers. The climbing fibers could mediate a signal related to image slip, similar to that in the flocculus (Stone and Lisberger 1989). This image slip signal could trigger the postulated dump switch that initiates rapid loss of horizontal eye velocity during per- or postrotatory nystagmus or OKAN in monkeys when they are exposed to a self-stationary visual surround (Raphan et al. 1979; Waespe et al. 1985).

The model simulated OKN and OKAN in upright and tilted positions in the normal state and after partial and complete nodulo-uvulectomy (Fig. 19). After partial or complete lesions, centrifugation would tilt the GIA vector, but because the rotation is around the head vertical, the nystagmus would be horizontal. The horizontal time constant would be independent of the magnitude of GIA tilt, just as yaw axis OKAN was independent of gravity for any head position. Rapid reorientation after nodulo-uvulectomy would also not result in any shift in yaw axis postrotatory nystagmus. It should be noted that the stimuli in these conditions were along the cardinal axes. If OKN were oblique with respect to the monkey after either partial or complete lesions, however, the OKAN would tend toward the horizontal, which has the longer time constant.

The model leads to the postulate that Purkinje cells in Zones 1 and 2 modulate anterior and posterior canal-related VO neurons in peripheral SVN, to control the vertical and roll time constants, and the horizontal to vertical (h_{13}) and horizontal to roll (h_{23}) cross-coupling parameters. The parameter h_{13}, for example, determines the extent to which input signals aligned with the *Z*-axis of the head will excite the vertical mode of velocity storage. Purkinje cells in Zone 3 modulate lateral canal-related VO neurons in MVN_p, to control the horizontal time constant, $1/h_{33}$. As a result, horizontal VO neurons, which are believed responsible for the generation of velocity storage (Holstein et al. 1996; Reisine and Raphan 1992; Wearne et al. 1997a; Yokota et al. 1992), are likely to provide the activity that drives the vertical VO neurons during cross coupling. Thus the three-D *H* matrix of the velocity storage mechanism is probably realized by interconnections of horizontal and vertical VO neurons in the vestibular nuclei.

The model also predicts that vertical VO neurons are activated concurrently with horizontal VO neurons from the onset of stimulation. This is supported by the early onset of cross-coupling at the beginning of yaw axis OKN or during horizontal nystagmus induced by electrical stimulation of the nucleus of the optic tract or of the vestibular nuclei when delivered with the head in tilted positions (Dai et al. 1991; Gizzi et al. 1994; Schiff et al. 1988; Yokota et al. 1992).

Finally, it is postulated that to control cross-coupling, the nodulus and uvula must govern the information flow from horizontal to vertical VO neurons, as shown by the arrows through h_{13} and h_{23}. Because Purkinje cells are inhibitory, and because the VO neurons may also be GABAergic (Holstein et al. 1996), disinhibition is likely to be a fundamental excitatory process in controlling the spatial orientation properties of velocity storage. By contrast, control of the horizontal time constant is likely to be accomplished by an inhibitory projection from Purkinje cells in the nodulus and sublobule 9d to horizontal VO neurons.

In summary, we have shown that the three-dimensional

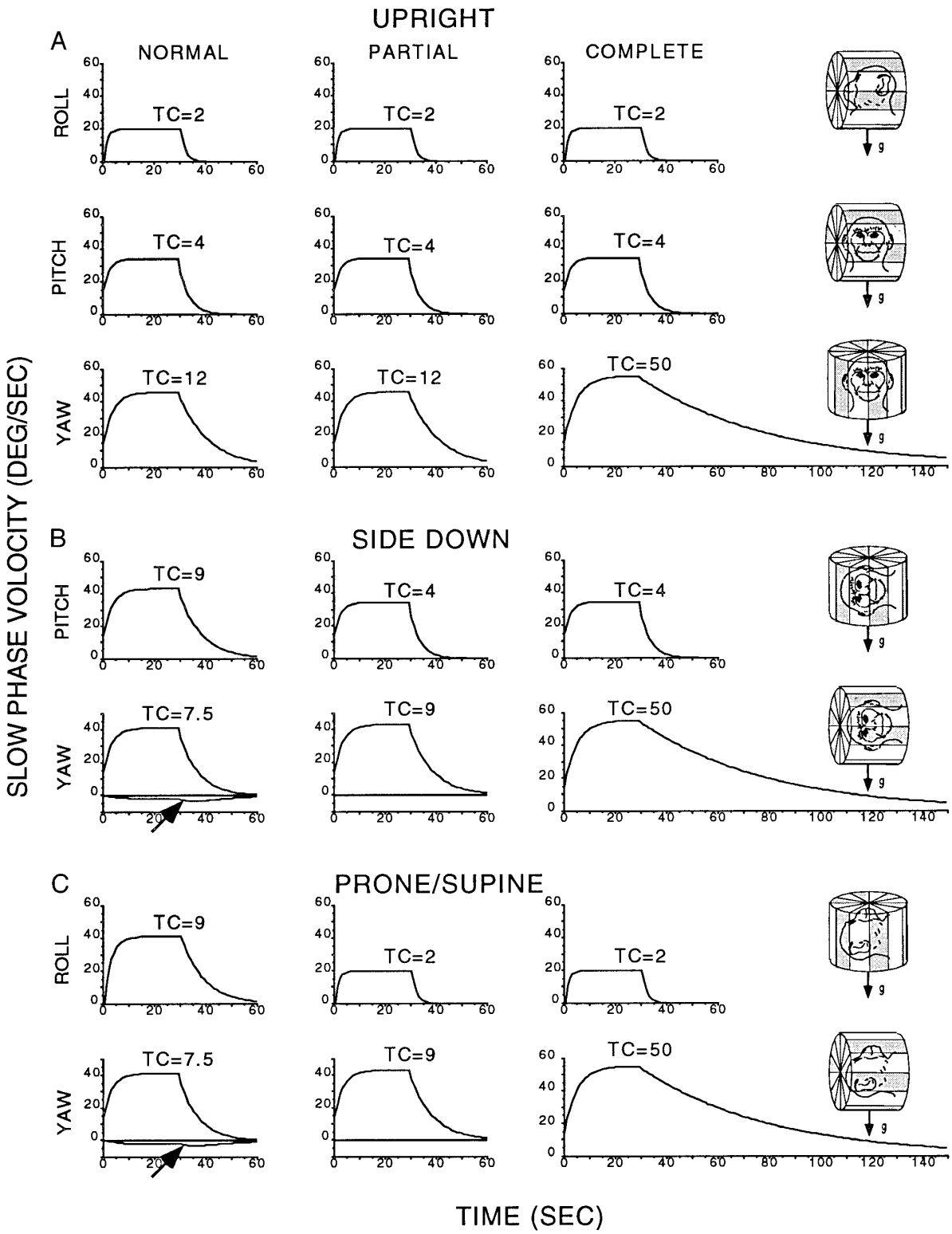

FIG. 19. Model simulations of the roll, pitch, and yaw slow-phase velocities induced by roll, pitch, and yaw stimulation with the animal upright (*A*), on-side (*B*), and prone/supine (*C*). The *1st column* are normal responses, the *2nd* and *3rd columns* are responses after partial and complete nodulo-uvulectomy. The direction of gravity is denoted by g. The large upward arrows in *B* and *C* refer to cross-coupled vertical and roll velocities, respectively. See text for further details.

dynamics of the velocity storage system are determined by the nodulus and ventral uvula. We propose that vertical and roll components of the cross-coupled response are modulated by central portions of the nodulus and ventral uvula, whereas the horizontal time constant is controlled by lateral portions of the nodulus. Together, these control mechanisms provide

a behavioral correlate for functional specificity of individual zones of these parts of the vestibulocerebellum in controlling spatial orientation and posture.

We thank Drs. Gay R. Holstein and Jean Büttner-Ennever for helping with anatomic sectioning and analysis. We thank Dr. Jan Voogd for providing anatomic data and measurements relating to the structural organization of the rhesus monkey nodulus and ventral uvula. We are grateful to Dr. Walter Waespe for providing some of the data used in this study. V. Rodriguez made an outstanding contribution assisting in the operations and in producing the figures.

This work was supported by National Institutes of Health Grants NS-00294, EY-11812, EY-04148, EY-01867, and DC-09284.

Address for reprint requests: B. Cohen, Dept. of Neurology, Box 1135, Mount Sinai School of Medicine, 1 Gustave L. Levy Place, New York, NY 10029.

Received 30 August 1997; accepted in final form 22 January 1998.

REFERENCES

ALLEY, K., BAKER, R., AND SIMPSON, J. I. Afferents to the vestibulo-cerebellum and the origin of the visual climbing fibers in the rabbit. *Brain Res.* 98: 582–589, 1975.

ANGAUT, P. AND BRODAL, A. The projections of the ''vestibulocerebellum'' onto the vestibular nuclei in the cat. *Arch. Ital. Biol.* 105: 441–479, 1967.

ANGELAKI, D. E. AND HESS, B.J.M. The cerebellar nodulus and ventral uvula control the torsional vestibulo-ocular reflex. *J. Neurophysiol.* 72: 1443–1447, 1994a.

ANGELAKI, D. E. AND HESS, B.J.M. Inertial representation of angular motion in the vestibular system of rhesus monkeys. I. Vestibuloocular reflex. *J. Neurophysiol.* 71: 1222–1249, 1994b.

ANGELAKI, D. E. AND HESS, B.J.M. Inertial representation of angular motion in the vestibular system of rhesus monkeys. II. Otolith-controlled transformation that depends on an intact cerebellar nodulus. *J. Neurophysiol.* 73: 1729–1751, 1995.

BALABAN, C. D. AND HENRY, R. T. Zonal organization of olivo-nodulus projections in albino rabbits. *Neurosci. Res.* 5: 409–423, 1988.

BARMACK, N. H., BAUGHMAN, R. W., ERRICO, P., AND SHOJAKU, H. Vestibular primary afferent projections to the cerebellum of the rabbit. *J. Comp. Neurol.* 327: 521–534, 1993a.

BARMACK, N. H., FAGERSON, M., FREDETTE, B. J., MUGNAINI, E., AND SHOJAKU, H. Activity of neurons in the beta nucleus of the inferior olive of the rabbit evoked by natural vestibular stimulation. *Exp. Brain Res.* 94: 203–215, 1993b.

BARMACK, N. H. AND FAGERSON, M. H. Vestibularly-evoked activity of single neurons in the dorsomedial cell column of the inferior olive in rabbit. *Soc. Neurosci. Abstr.* 20: 1190, 1994.

BARMACK, N. H., MUGNAINI, E., AND NELSON, B. J. Vestibularly-evoked activity of single neurons in the beta nucleus of the inferior olive. In: *The Olivocerebellar System in Motor Control*, edited by P. Strata. Berlin: Springer-Verlag, 1989, p. 313–322.

BARMACK, N. H. AND SHOJAKU, H. Representation of a postural coordinate system in the nodulus of the rabbit cerebellum by vestibular climbing fiber signals. In: *Vestibular and Brain Stem Control of Eye, Head, and Body Movement*, edited by H. Shimazu and Y. Shinoda. Tokyo: Japan Scientific Societies Press, 1992, p. 331–338.

BARMACK, N. H. AND SHOJAKU, H. Vestibular and visual climbing fiber signals evoked in the uvula-nodulus of the rabbit cerebellum by natural stimulation. *J. Neurophysiol.* 74: 2573–2589, 1995.

BENSON, A. J. Modification of the response to angular accelerations by linear accelerations. In: *Handbook of Sensory Physiology*, edited by H. Kornhuber. Berlin: Springer, 1974, vol. VI, p. 281–320.

BLANKS, R.H.I., CURTHOYS, I. S., BENNET, M., AND MARKHAM, C. H. Planar relationships of the semicircular canals in rhesus and squirrel monkeys. *Brain Res.* 340: 315–324, 1985.

BLES, W., DE JONG, J.M.B.V., AND DE WIT, G. Somatosensory compensation for loss of vestibular function. *Acta Otolaryngol. (Stockh)*. 97: 213–221, 1984.

BOWER, J. M. AND WOOLSTON, D. C. Congruence of spatial organization of tactile projections to granule cell and Purkinje cell layers of cerebellar hemispheres of the albino rat: vertical organization of the cerebellar cortex. *J. Neurophysiol.* 49: 745–766, 1983.

BRODAL, A. AND BRODAL, P. Observations on the secondary vestibulocerebellar projections in the macaque monkey. *Exp. Brain. Res.* 58: 62–74, 1985.

BRODAL, A. AND HOIVIK, G. H. Site and mode of termination of primary vestibulocerebellar fibres in the cat. An experimental study with silver impregnation methods. *Arch. Ital. Biol.* 102: 1–21, 1964.

COHEN, B. Spatial orientation of the angular vestibulo-ocular reflex. *J. Vestib. Res.* In press.

COHEN, B., HELWIG, D., AND RAPHAN, T. Baclofen and velocity storage: a model of the effects of the drug on the vestibulo-ocular reflex in the rhesus monkey. *J. Physiol. (Lond.)* 393: 703–725, 1987.

COHEN, B., HENN, V., RAPHAN, T., AND DENNETT, D. Velocity storage, nystagmus, and visual vestibular interactions in humans. *Ann. NY Acad. Sci.* 374: 421–433, 1981.

COHEN, B., MATSUO, V., AND RAPHAN, T. Quantitative analysis of the velocity characteristics of optokinetic nystagmus and optokinetic after-nystagmus. *J. Physiol. (Lond.)* 270: 321–344, 1977.

COHEN, H., COHEN, B., RAPHAN, T., AND WAESPE, W. Habituation and adaptation of the vestibulo-ocular reflex: a model of differential control by the vestibulo-cerebellum. *Exp. Brain Res.* 90: 526–538, 1992.

DAI, M., MCGARVIE, L., KOZLOVSKAYA, I. B., RAPHAN, T., AND COHEN, B. Effects of spaceflight on ocular counterrolling and spatial orientaion of the vestibular system. *Exp. Brain Res.* 102: 45–56, 1994.

DAI, M., RAPHAN, T., AND COHEN, B. Spatial orientation of the vestibular system: dependence of optokinetic after nystagmus on gravity. *J. Neurophysiol.* 66: 1422–1438, 1991.

DAI, M. J., RAPHAN, T., AND COHEN, B. Characterization of yaw to roll cross-coupling in the three-dimensional structure of the velocity storage integrator. *Ann. NY Acad. Sci.* 656: 140–157, 1992.

ENGELKEN, E. J. AND STEVENS, K. W. A new approach to the analysis of nystagmus: an application for order statistic filters. *Aviat. Space Environ. Med.* 61: 859–864, 1990.

ENGELKEN, E. J. AND STEVENS, K. W. Optimization of an adaptive nonlinear filter for the analysis of nystagmus. *Rocky Mountain Bioengineering Symposium 1991.*

FETTER, M., TWEED, D., HERMANN, B., WOHLAND-BRAUN, B., AND KOENIG, E. The influence of head position and head reorientation on the axis of eye rotation and the vestibular time constant during postrotatory nystagmus. *Exp. Brain Res.* 99: 121–128, 1992.

FUCHS, A. F. AND KIMM, J. Unit activity in the vestibular nucleus of the alert monkey during horizontal angular acceleration and eye movement. *J. Neurophysiol.* 38: 1140–1161, 1975.

GIZZI, M., RAPHAN, T., RUDOLPH, S., AND COHEN, B. Orientation of human optokinetic nystagmus to gravity: a model based approach. *Exp. Brain Res.* 99: 347–360, 1994.

GOLDBERG, J. M. AND FERNANDEZ, C. Physiology of peripheral neurons innervating semicircular canals of the squirrel monkey. I. Resting discharge and response to angular accelerations. *J. Neurophysiol.* 34: 635–660, 1971.

GOLDSTEIN, H. *Classical Mechanics.* Reading, MA: Addison-Wesley, 1980.

GRAF, W., SIMPSON, J. I., AND LEONARD, C. S. The spatial organization of visual messages in the flocculus of the rabbit's cerebellum. II. Complex and simple spike responses of Purkinje cells. *J. Neurophysiol.* 60: 2091–2121, 1988.

GUEDRY, F. E. Psychophysics of vestibular sensation. In: *Handbook of Sensory Physiology*, edited by H. H. Kornhuber. New York: Springer Verlag, 1974, vol. 6, p. 3–154.

HAINES, D. E. Cerebellar corticonuclear and corticovestibular fibers of the flocculonodular lobe in a prosimian primate (*Galago senegalensis*). *J. Comp. Neurol.* 174: 607–630, 1977.

HALMAGYI, G. M., RUDGE, P., GRESTY, M. A., LEIGH, J. R., AND ZEE, D. S. Treatment of periodic alternating nystagmus. *Ann. Neurol.* 8: 609–611, 1980.

HARRIS, L. R. Vestibular and optokinetic eye movements evoked in the cat by rotation about a tilted axis. *Exp. Brain Res.* 66: 522–532, 1987.

HARRIS, L. R. AND BARNES, G. R. Orientation of vestibular nystagmus is modified by head tilt. In: *The Vestibular System: Neurophysiologic and Clinical Research*, edited by M. D. Graham and J. L. Kemink. New York: Raven, p. 539–548, 1987.

HEINEN, S. J. AND KELLER, E. L. The function of the cerebellar uvula in monkey during optokinetic and pursuit eye movements: single-unit responses and lesion effects. *Exp. Brain Res.* 110: 1–14, 1996.

HEINEN, S. J., OH, D. K., AND KELLER, E. L. Characteristics of nystagmus

evoked by electrical stimulation of the uvular/nodular lobules of the cerebellum in monkey. *J. Vestib. Res.* 2: 233–245, 1992.

HELMHOLTZ, H. V. *Handbuch der physiologischen Optik. Leipzig: Voss. English translation: Treatise on Physiological Optics.* New York: Dover (1962), 1866.

HOLSTEIN, G. R., MARTINELLI, G. P., DEGEN, J., AND COHEN, B. Inhibitory neuronal circuits in the central vestibular system. *Ann. NY Acad. Sci.* 781: 443–457, 1996.

ITO, M. *The Cerebellum and Neural Control*. New York: Raven, 1984.

JUDGE, S. J., RICHMOND, B. J., AND CHU, F. C. Implantation of magnetic search coils for measurement of eye position: an improved method. *Vision Res.* 20: 535–538, 1980.

KANO, M., KANO, M. S., KUSUNOKI, M., AND MAEKAWA, K. Nature of optokinetic response and zonal organization of climbing fiber afferents in the vestibulocerebellum of the pigmented rabbit. II. The nodulus. *Exp. Brain Res.* 80: 238–251, 1990.

KATAYAMA, S. AND NISIMARU, N. Parasagittal zonal pattern of olivo-nodular projection in rabbit cerebellum. *Neurosci. Res.* 5: 424–438, 1988.

KATZ, E., DE JONG, J.M.B.V., BÜTTNER-ENNEVER, J. A., AND COHEN, B. Effects of midline medullary lesions on velocity storage and the vestibulo-ocular reflex. *Exp. Brain Res.* 87: 505–520, 1991.

LEIGH, R. J., ROBINSON, D. A., AND ZEE, D. S. A hyptothetical explanation for periodic alternating nystagmus: instability in the optokinetic-vestibular system. *Ann. NY Acad. Sci.* 374: 619–635, 1981.

LEONARD, C. S., SIMPSON, J. I., AND GRAF, W. The spatial organization of visual messages in the flocculus of the rabbit's cerebellum. I. Typology of inferior olive neurons of the dorsal cap of Kooy. *J. Neurophysiol.* 60: 2073–2090, 1988.

MADIGAN, J. AND CARPENTER, M. *Cerebellum of the Rhesus Monkey. Atlas of Lobules, Laminae and Folia in Sections.* London: University Park Press, 1971.

MARINI, G., PROVINI, L., AND ROSINA, A. Macular input to the cerebellar nodulus. *Brain Res.* 99: 367–371, 1975.

MATSUO, V. AND COHEN, B. Vertical optokinetic nystagmus and vestibular nystagmus in the monkey: up-down asymmetry and effects of gravity. *Exp. Brain Res.* 53: 197–216, 1984.

MATSUO, V., COHEN, B., RAPHAN, T., DEJONG, V., AND HENN, V. Asymmetric velocity storage for upward and downward nystagmus. *Brain Res.* 176: 159–164, 1979.

MERFELD, D. M. Modeling the vestibulo-ocular reflex of the squirrel monkey during eccentric rotation and roll tilt. *Exp. Brain Res.* 106: 123–134, 1995.

MERFELD, D. M., YOUNG, L. R., OMAN, C. M., AND SHELHAMER, M. J. A multidimensional model of the effect of gravity on the spatial orientation of the monkey. *J. Vestib. Res.* 3: 141–161, 1993.

OSCARSSON, O. The sagittal organization of the cerebellar anterior lobe as revealed by the projection patterns of the climbing fiber system. In: *Neurobiology of Cerebellar Evolution and Development*, edited by R. Llinas. Chicago, IL: American Medical Association, 1969, p. 525–537.

OSCARSSON, O. Functional units of the cerebellum—sagittal zones and microzones. *Trends Neurosci.* 2: 143–145, 1979.

PRECHT, W., SIMPSON, J. I., AND LLINAS, R. Responses of Purkinje cells in rabbit nodulus and uvula to natural vestibular and visual stimuli. *Pflügers Arch.* 367: 1–6, 1976.

RAPHAN, T. AND COHEN, B. Multidimensional organization of the vestibulo-ocular reflex (VOR). In: *Adaptive Processes in Visual and Oculomotor System*, edited by E. L. Keller and D. S. Zee. New York: Pergamon, 1986, p. 285–292.

RAPHAN, T. AND COHEN, B. Organizational principles of velocity storage in three dimensions: the effect of gravity on cross-coupling of optokinetic after-nystagmus. *Ann. NY Acad. Sci.* 545: 74–92, 1988.

RAPHAN, T. AND COHEN, B. How does the vestibulo-ocular reflex work? In: *Disorders of the Vestibular System*, edited by R. W. Baloh and G. M. Halmagyi. New York: Oxford Univ. Press, 1996, p. 20–47.

RAPHAN, T., COHEN, B., AND HENN, V. Effects of gravity on rotatory nystagmus in monkeys. *Ann. NY Acad. Sci.* 374: 44–55, 1981.

RAPHAN, T., DAI, M., AND COHEN, B. Spatial orientation of the vestibular system. *Ann. NY Acad. Sci.* 656: 140–157, 1992.

RAPHAN, T., MATSUO, V., AND COHEN, B. Velocity storage in the vestibulo-ocular reflex arc (VOR). *Exp. Brain Res.* 35: 229–248, 1979.

RAPHAN, T. AND STURM, D. Modelling the spatiotemporal organization of velocity storage in the vestibuloocular reflex by optokinetic studies. *J. Neurophysiol.* 66: 1410–1420, 1991.

RAPHAN, T., WEARNE, S., AND COHEN, B. Modeling the organization of the linear and angular vestibulo-ocular reflexes. *Ann. NY Acad. Sci.* 781: 348–363, 1996.

REISINE, H. AND RAPHAN, T. Neural basis for eye velocity generation in the vestibular nuclei during off-vertical axis rotation. *Exp. Brain Res.* 92: 209–226, 1992.

ROBINSON, D. A. A method of measuring eye movement using a scleral search coil in a magnetic field. *IEEE Trans. Biomed. Electron.* 10: 137–145, 1963.

ROBINSON, D. A. The use of matrices in analyzing the three dimensional behavior of the vestibulo-ocular reflex. *Biol. Cybern.* 46: 53–66, 1982.

SCHIFF, D., COHEN, B., AND RAPHAN, T. Nystagmus induced by stimulation of the nucleus of the optic tract in the monkey. *Exp. Brain Res.* 70: 1–14, 1988.

SHOJAKU, H., BARMACK, N. H., AND MIZUKOSHI, K. Influence of vestibular and visual climbing fiber signals on Purkinje cell discharge in the cerebellar nodulus of the rabbit. *Acta Otolaryngol. Suppl. (Stockh.)* 481: 242–246, 1991.

SHOJAKU, H., SATO, Y., IKARASHI, K., AND KAWASAKI, T. Topographical distribution of Purkinje cells in the uvula and the nodulus projecting to the vestibular nuclei in cats. *Brain Res.* 416: 100–112, 1987.

SIMPSON, J. I. AND ALLEY, K. E. Visual climbing fiber input to rabbit vestibulo-cerebellum: a source of direction-specific information. *Brain Res.* 82: 302–308, 1974.

SIMPSON, J. I. AND GRAF, W. The selection of reference frames by nature and its investigators. In: *Adaptive Mechanisms in Gaze Control; Reviews of Oculomotor Research*, edited by A. Berthoz and G. M. Jones. Amsterdam: Elsevier, 1985, vol. 1, p. 3–16.

SIMPSON, J. I., GRAF, W., AND LEONARD, C. The coordinate system of visual climbing fibers to the flocculus. In: *Progress in Oculomotor Research*, edited by A. F. Fuchs and W. Becker. New York: Elsevier, 1981, p. 475–484.

SNIDER, R. S. AND LEE, J. C. *A Stereotaxic Atlas of the Monkey Brain (Macaca mulatta)*. Chicago, IL: Univ. Chicago Press, 1961.

SOLOMON, D. AND COHEN, B. Stabilization of gaze during circular locomotion in darkness. II. Contribution of velocity storage to compensatory eye and head nystagmus in the running monkey. *J. Neurophysiol.* 67: 1158–1170, 1992.

SOLOMON, D. AND COHEN, B. Stimulation of the nodulus and uvula discharges velocity storage in the vestibulo-ocular reflex. *Exp. Brain Res.* 102: 57–68, 1994.

STONE, L. S. AND LISBERGER, S. G. Synergic action of complex and simple spikes in the monkey flocculus in the control of smooth-pursuit eye movement. *Exp. Brain Res. Suppl.* 17: 299–312, 1989.

TAKEDA, T. AND MAEKAWA, K. Collateralized projection of visual climbing fibers to the flocculus and nodulus of the rabbit. *Neurosci. Res.* 2: 125–132, 1984.

TAN, J., GERRITS, N. M., NANHOE, R., SIMPSON, J. I., AND VOOGD, J. Zonal organization of the climbing fiber projection to the flocculus and nodulus of the rabbit. A combined axonal tracing and acetylcholinesterase histochemical study. *J. Comp. Neurol.* 356: 23–50, 1995.

TWEED, D. AND VILIS, T. Geometric relations of eye position and velocity vectors during saccades. *Vision Res.* 30: 111–127, 1990.

UEMURA, T. AND COHEN, B. Effects of vestibular nuclei lesion on vestibulo-ocular reflexes and posture in monkeys. *Acta Otolaryngol. Suppl.* 315: 1–71, 1973.

VAN OPSTAL, A. J., HEPP, K., SUZUKI, Y., AND HENN, V. Influence of eye position on activity in monkey superior colliculus. *J. Neurophysiol.* 74: 1593–1610, 1995.

VOOGD, J. *The Cerebellum of the Cat. Structure and Fibre Connexions* Philadelphia, PA: F.A. Davies, 1964.

VOOGD, J. The importance of fiber connections in the comparative anatomy of the mammalian cerebellum. In: *Neurobiology of Cerebellar Evolution and Development*, edited by R. Llinas. Chigaco, IL: AMA, 1969, p. 493–514.

VOOGD, J. AND BIGARÉ, F. Topographical distribution of olivary and corticonuclear fibers in the cerebellum. A review. In: *The Inferior Olivary Nucleus: Anatomy and Physiology*, edited by J. Courville, C.C.D. Montigny, and Y. Lamarre. New York: Raven, 1980, p. 207–234.

VOOGD, J., GERRITS, N. M., AND RUIGROK, T.J.H. Organization of the vestibulocerebellum. *Ann. NY Acad. Sci.* 781: 553–579, 1996.

WAESPE, W., COHEN, B., AND RAPHAN, T. Role of the flocculus and paraflocculus in optokinetic nystagmus and visual-vestibular interaction: Effects of lesions. *Exp. Brain Res.* 50: 9–33, 1983.

WAESPE, W., COHEN, B., AND RAPHAN, T. Dynamic modification of the

vestibulo-ocular reflex by the nodulus and uvula. *Science* 228: 199–201, 1985.

WALBERG, F. AND DIETRICHS, E. The interconnection between the vestibular nuclei and the nodulus: a study of reciprocity. *Brain Res.* 449: 47–53, 1988.

WEARNE, S., COHEN, B., AND RAPHAN, T. Nodulo-uvular control of central vestibular dynamics determines spatial orientation of the angular vestibulo-ocular reflex. *Ann. NY Acad. Sci.* 781: 364–384, 1996.

WEARNE, S., RAPHAN, T., AND COHEN, B. Contribution of vestibular commissural pathways to velocity storage and spatial orientation of the angular vestibulo-ocular reflex. *J. Neurophysiol.* 78: 1193–1197, 1997a.

WEARNE, S., RAPHAN, T., AND COHEN, B. Compensatory and orienting components of the vestibulo-ocular reflex during centrifugation. *J. Neurophysiol.* 1997b.

WYLIE, D. R., DE ZEEUW, C. I., DIGIORGI, P. L., AND SIMPSON, J. I. Projections of individual Purkinje cells of identified zones in the ventral nodulus to the vestibular and cerebellar nuclei in the rabbit. *J. Comp. Neurol.* 349: 448–463, 1994.

YAKUSHIN, S. B., DAI, M. J., SUZUKI, J.-I., RAPHAN, T., AND COHEN, B. Semicircular canal contribution to the three-dimensional vestibulo-ocular reflex: a model-based approach. *J. Neurophysiol.* 74: 2722–2738, 1995.

YATES, B. J. Vestibular influences on the sympathetic nervous system. *Brain Res. Rev.* 17: 51–59, 1992.

YATES, B. J., JAKUS, J., AND MILLER, A. D. Vestibular effects on respiratory outflow in the decerebrate cat. *Brain Res.* 629: 209–217, 1993.

YOKOTA, J. I., REISINE, H., AND COHEN, B. Nystagmus induced by electrical microstimulation of the vestibular and prepositus hypoglossi nuclei in the monkey. *Exp. Brain Res.* 92: 123–138, 1992.